

5.1 Ammonia

5.1.1 Sources, Emission inventories

Sampling methods gaseous and particulate phases

5.1.2 Gas-phase chemistry

5.1.3 Particle formation (nucleation)

5.1.4 Ammonia air/sea exchange

5.1.4.1 Equilibria

5.1.4.2 Fluxes

5.1.5 Ammonia surface fluxes Flux measurement

(parts of chapter 9)

Ammonia (NH₃): Significance

- only common alkaline gas in the atmosphere: at least partly neutralisation of acidic particles, rain and cloudwater (however, returning acidity upon deposition to soil); discovered in rainwater (*de Saussure, 1804*)
- necessary for particle formation (ternary nucleation)

5.1.1 Sources

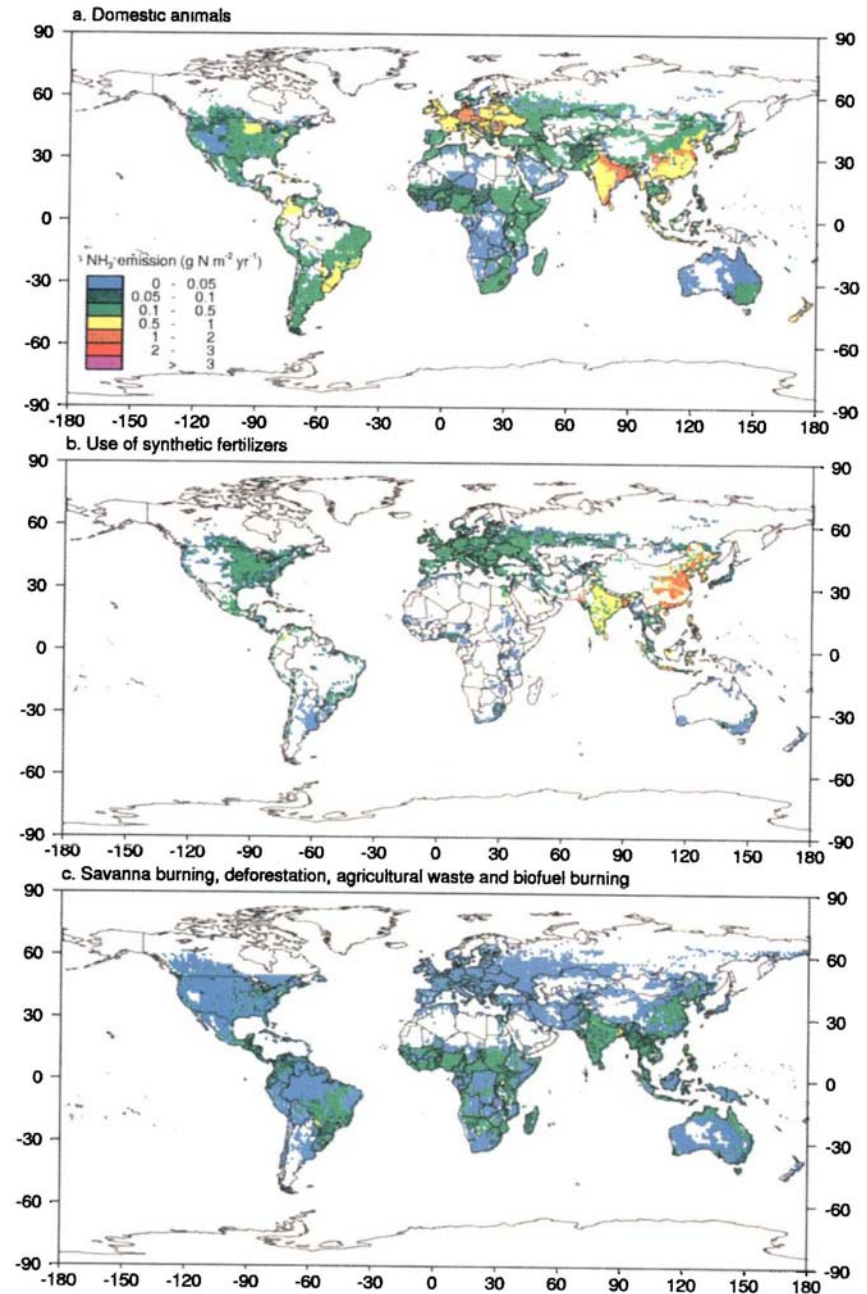
TABLE I. Yearly NH_3 emissions [Tg N yr^{-1}]

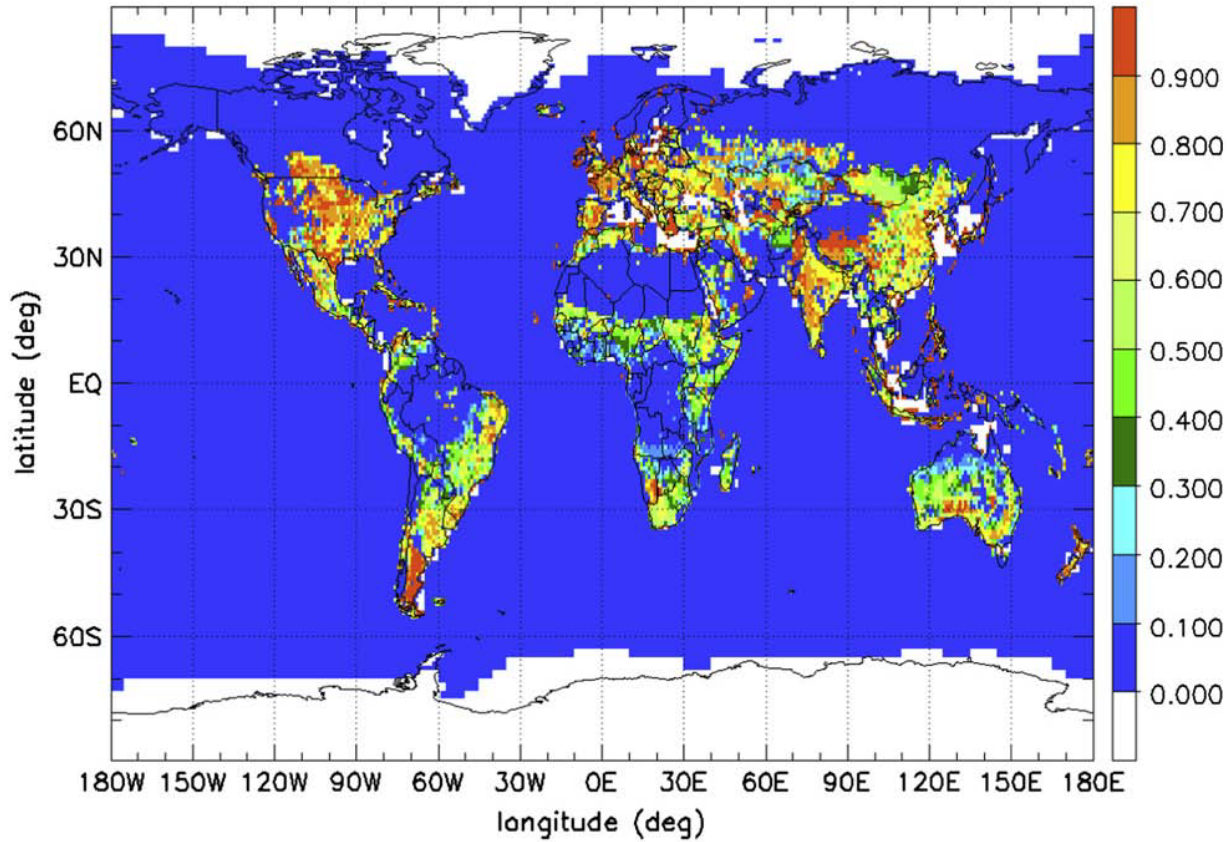
Anthropogenic:

dairy cattle	5.5
beef cattle/buffaloes	8.7
pigs	2.8
horses/mules/asses	1.2
sheep/goats	2.5
poultry	1.3
fertilizer	6.4
biomass burning	2.0
subtotal	30.4

Natural:

wild animals	2.5
vegetation	5.1
ocean	7.0
subtotal	14.6
Total	45.0





Fraction of ammonia emissions due to agricultural activities (*Sutton et al., 2008*)

Emission inventories: Methodology

Ingredients are

1. emission factors
2. time functions
3. spatial distributions

Table 1. Characteristics and N Excretion for Different Animal Categories for Two World Regions

Animal Category	Region	Animal Characteristics for Subclass ^a	N Excretion, kg head ⁻¹ yr ⁻¹	
			Subclass	Category
Dairy cattle	I	500 kg LW, 15 L milk d ⁻¹	80	80
	II	400 kg LW, 5 L milk d ⁻¹	60	60
Nondairy cattle	I	50% young cattle, 250 kg LW	30	45
		30% suckling cows, 500 kg LW, 10 L milk d ⁻¹	70	
	II	20% beef cattle 400 kg LW	25	40
		50% young cattle, 200 kg LW	25	
Buffalo	I and II	30% suckling cows, 400 kg LW, 5 L milk d ⁻¹	60	45
		20% draft cattle, 400 kg LW	40	
	I and II	40% female adult, 400 kg LW	60	45
		20% male adult, 500 kg LW	40	
Camels	I and II	20% young, 200 kg LW	30	55
		20% young, 400 kg LW	40	
	I and II	69% female adult, 500 kg LW	64	55
		3% male adult, 550 kg LW	40	
Horses	I and II	14% weaned, 187 kg LW	30	45
		14% immature, 356 kg LW	40	
Sheep	I and II	assumed equal to buffalo		10
Goats	I and II	based on 1 ewe and 1-1.5 adherent lambs		9
Pigs	I and II	assumed equal to 90% of sheep		11
		50% fattening pigs	14	
		10% sows	36	
Poultry	I and II	40% piglets and young sows	0	
		50% laying hens	0.6	0.5
		50% broilers	0.6	

Region I, developed countries (Europe, the former USSR, North America, Australia and New Zealand, Israel, and Japan); region II, developing countries (Latin America, Oceania excluding Australia and New Zealand, Africa, and Asia excluding the former USSR).

^a LW, live weight; percent, share of subclass in total of animal category.

1. Emission factors

Example NH₃ from agriculture:

Emissions from livestock have large regional differences, even within small countries:

- type, age, weight, and sex of animal
- manure, composition, liquid vs. dry (NH₃ only or not)
- ventilation, passive vs. Active
- type of stable

Aggregate via respective (statistical) distributions.

Klaassen, 1992

Bouwman et al., 1997

Sources NH₃ agriculture

Ammonia emission factors and total emissions for Switzerland

Emission factor (NH ₃ kg/animal/year)				
	Buijsman et al. (1987)	Stadelmann (1990)	Asman (1990)	Klaassen (1990)
Cattle	18	21.3	25.1	12.5 - 24.9
Pigs	2.8	2.1	4.8	4.8
Poultry	0.26	0.26	0.32	0.28 - 0.33
Horses	9.4	11.1	12.5	12.5
Sheep	3.1	2.7	1.9	2.1
Total agricultural emissions (kton NH ₃ per year)				
Reference year	1983	1987	1988	1987
	53	56	68 (63)*	55

N, P, K excreted per cow per month (standard cow with 5000 L milk/a and 600 kg live weight)

a) Standard values				
	N (kg)	P (kg)	K (kg)	m ³
per cow per month				
Average whole year	7.5	1.5	12	1.7
Summer rations (grass etc.)	8.6	1.5	13.8	1.9
Winter rations (hay, silage etc.)	6.2	1.5	9.7	1.4
b) Correction factors (%)				
Production level ± 1000 l milk per year	± 10	± 10	± 10	± 10
Basic forage ration grass + dried maize (summer)	- 11	- 5	- 8	- 6
Grass + silage (winter)	+ 3	+ 2	- 3	+ 5
Hay only (winter)	- 5	- 3	- 1	- 11
Sward composition				
Sward with few legumes	- 12	+ 4	- 8	--
Sward rich in legumes	+ 6	+ 4	+ 15	+ 1

Menzi et al., 1992

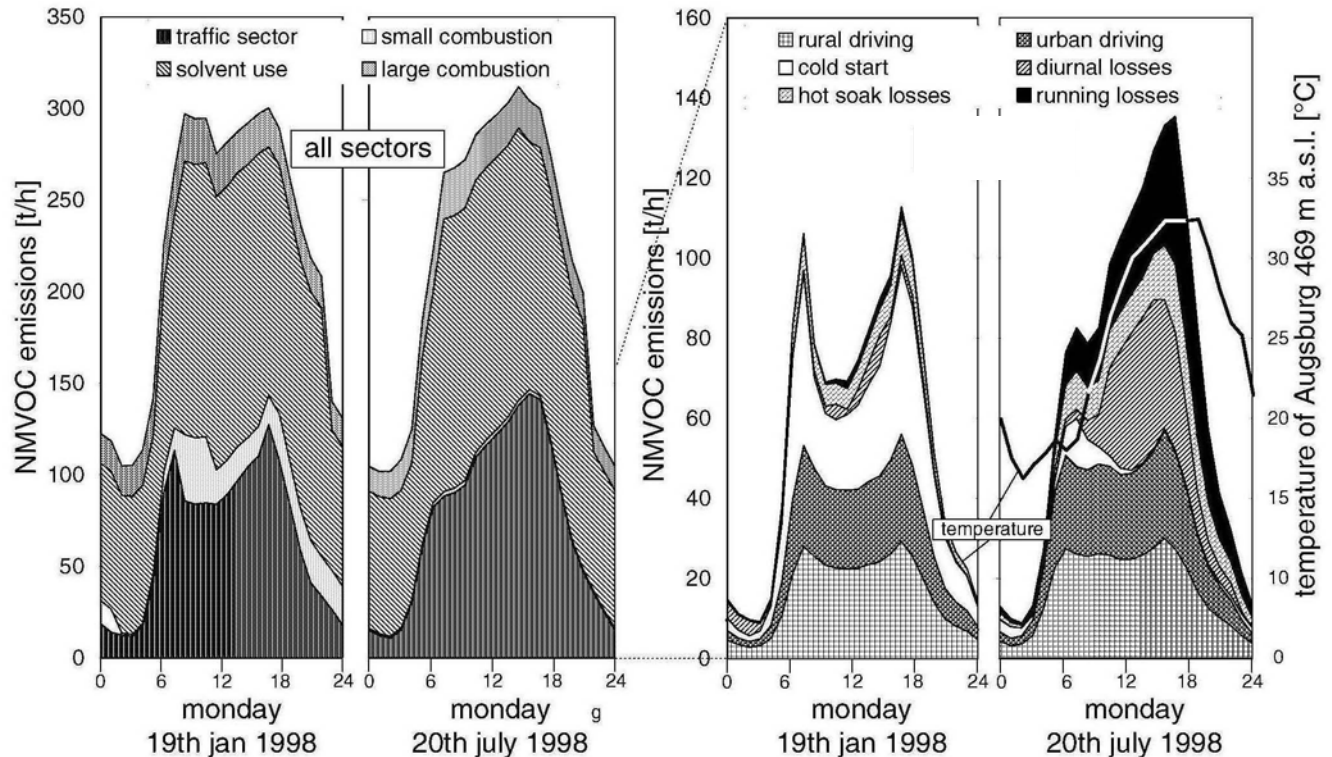
5-15% of fertilizer N applied reaches human, rest leaks into environment (*Erisman et al., 2007*)

Emission inventories: Methodology

2. Time functions

Example VOCs:

Measurement based diel, weekly etc. functions



All sectors

Traffic sector

Friedrich et al., 2002

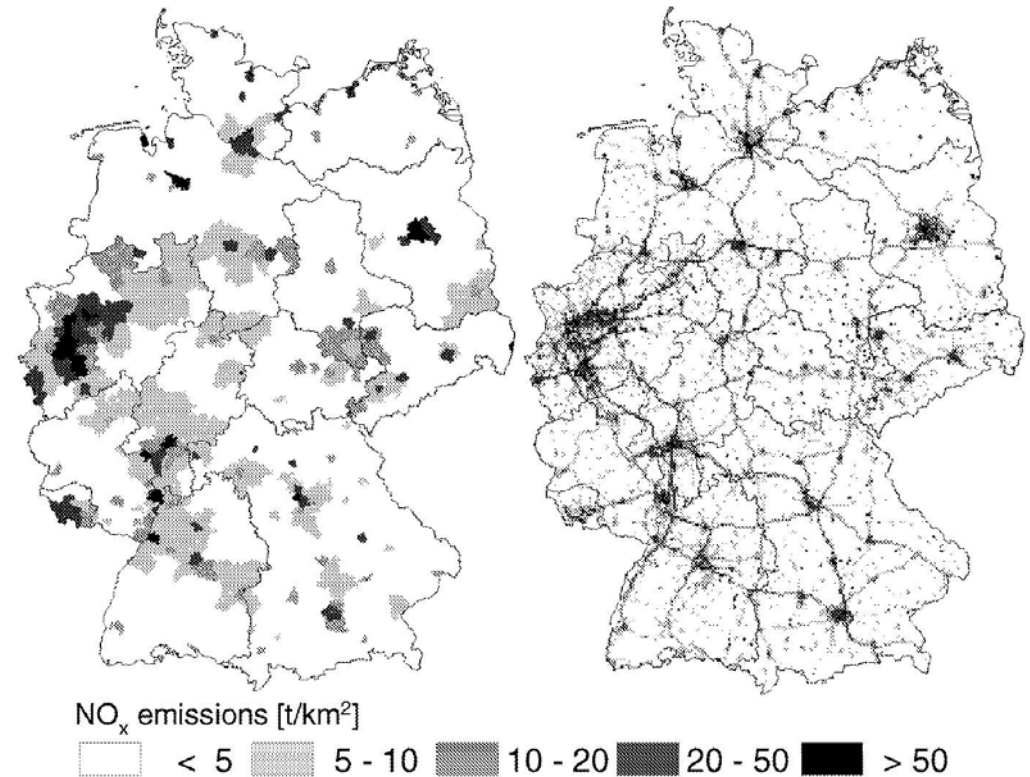
Emission inventories: Methodology

3. Spatial distributions

Example NO_x from road traffic:

Usually based on surrogate type of information:

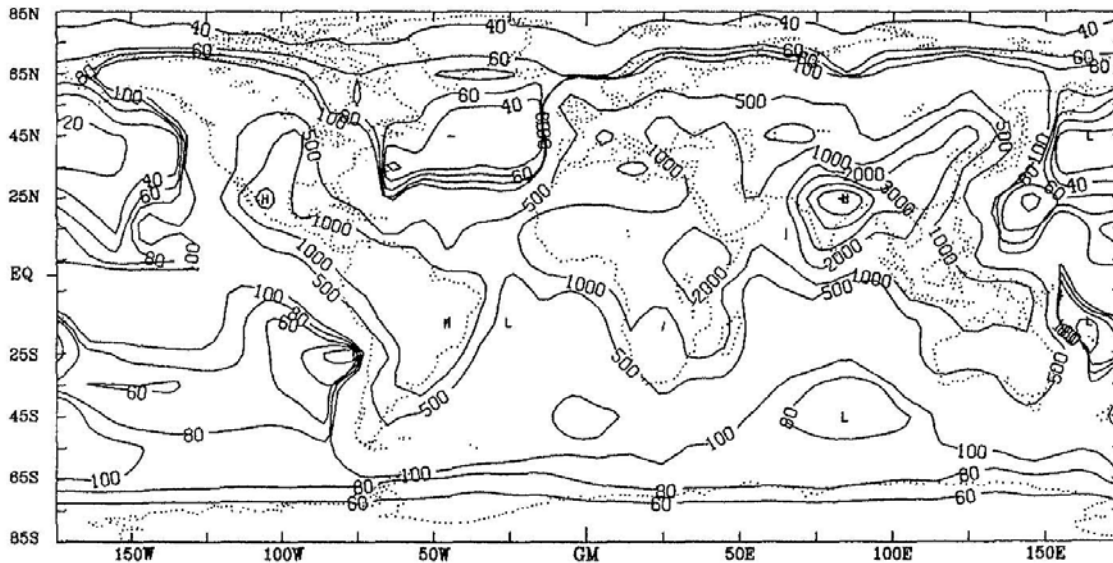
- land use categories
- population density
- gross domestic product per area



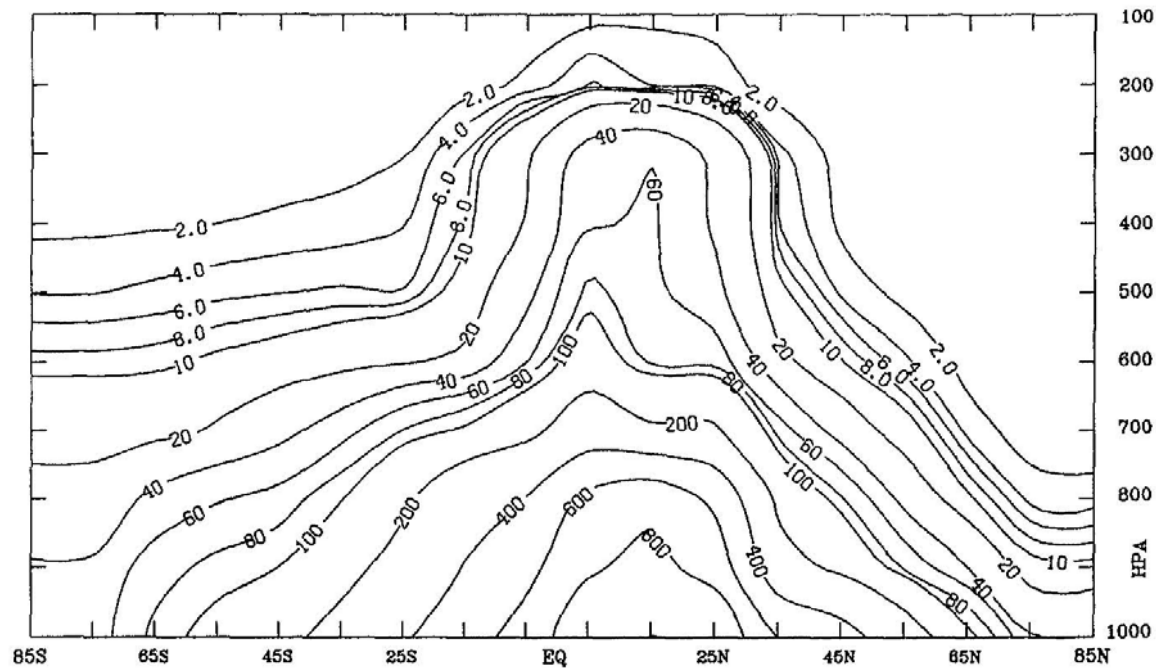
District level

3 km x 3 km grid level

Concentration distribution NH₃



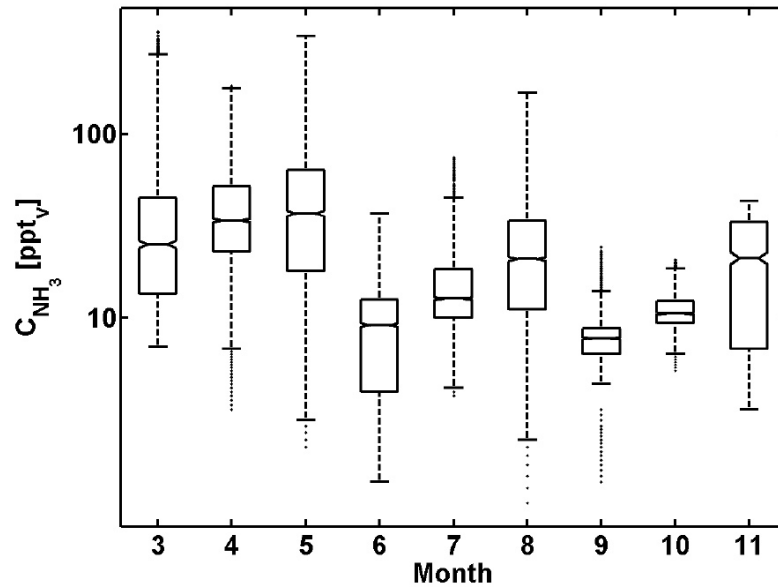
(pptv)



Dentener & Crutzen, 1994

Spatial variability is high

Extremes: E.g. very low in the boreal forest
(S Finland 2007; *Junninen et al., 2008*):

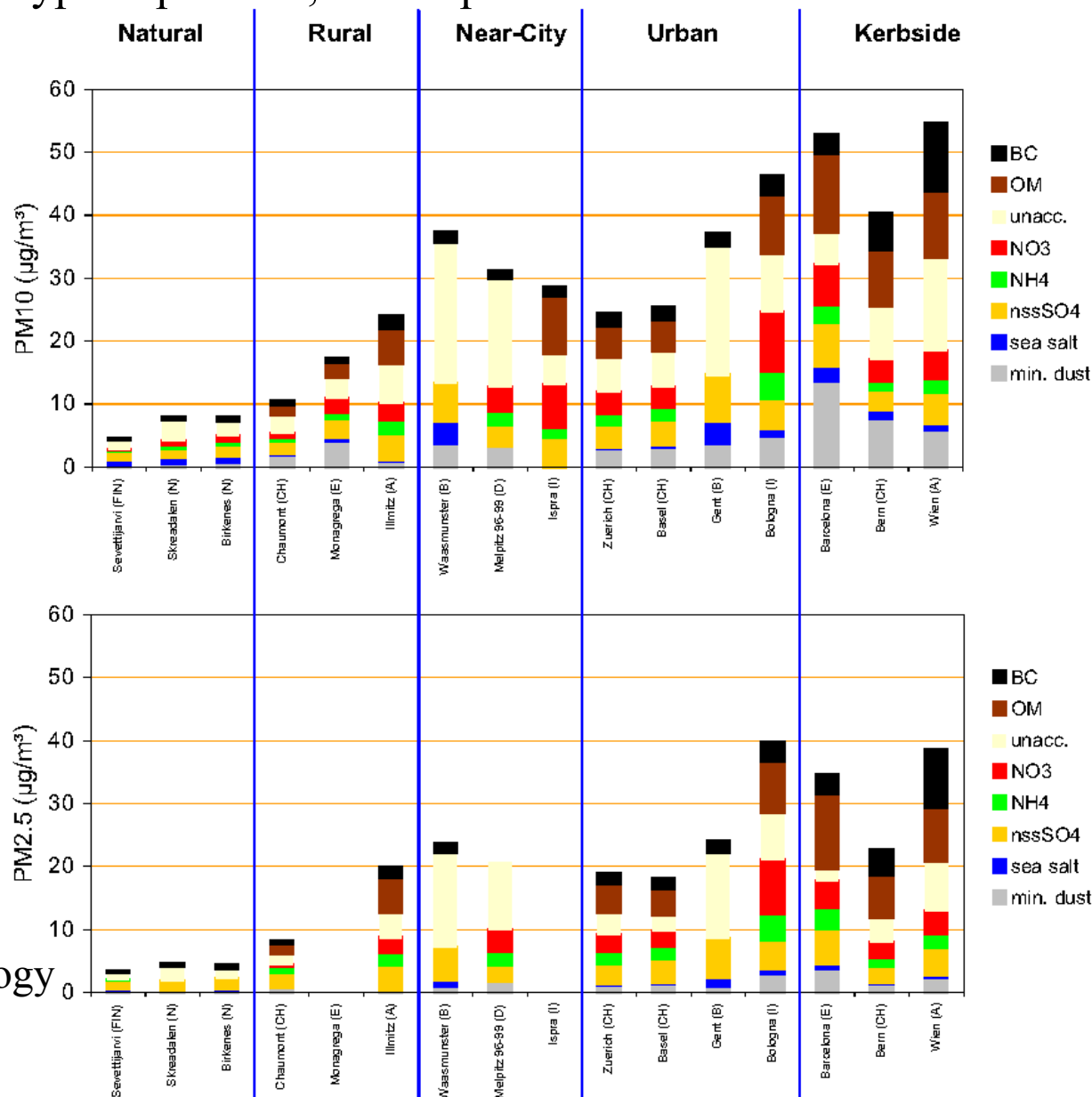


Revisited (→ 3.4.2.1):

Inorganic, major particulate phase components

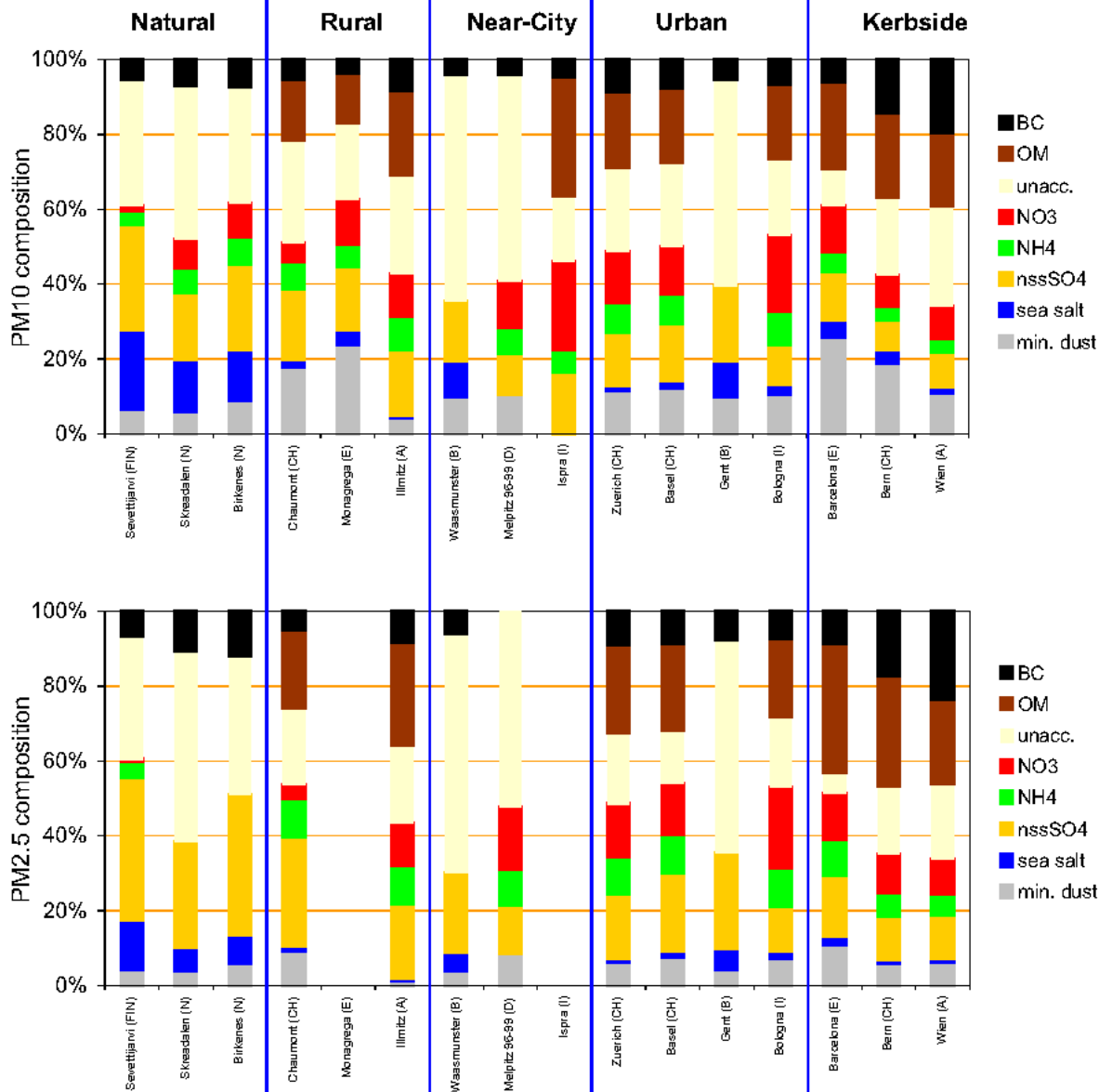
- site type dependent, size dependent

Concentration range
 NH_4^+



European aerosol phenomenology
(van Dingenen et al., 2004)

Revisited (→ 3.4.2.1):



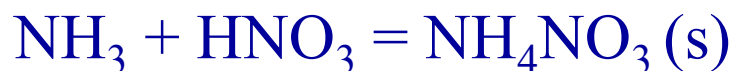
(van Dingenen et al., 2004)

Revisited (→ 3.4.3.1.1): N(-III) phase distribution in air

N(-III)/N(V) phase equilibrium

Temperature dependence

for $rh < rh_D$:



$$p_{\text{NH}_3} * p_{\text{HNO}_3} = \begin{array}{l} 0.12 \text{ ppbv}^2 (278 \text{ K}), \\ 2.0 \text{ ppbv}^2 (288 \text{ K}), \\ 28 \text{ ppbv}^2 (298 \text{ K}) \end{array}$$

Humidity dependence

for $rh > rh_D$:



gas-phase suppressed

most pronounced for low $\text{NO}_3^-/\text{SO}_4^{2-}$

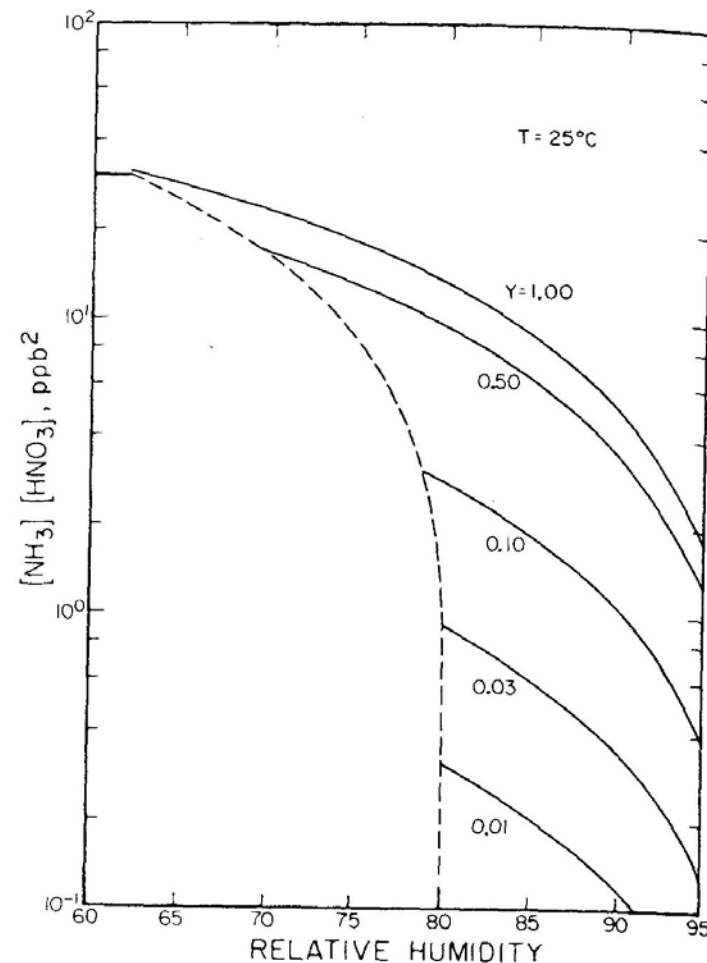


Fig. 2. The effect of $(\text{NH}_4)_2\text{SO}_4$ on the relative humidity dependence of the NH_4NO_3 dissociation constant.

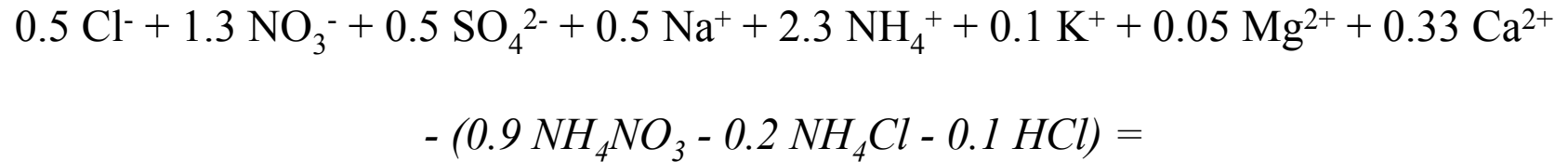
$$Y = \frac{[\text{NH}_4\text{NO}_3]}{\{[\text{NH}_4\text{NO}_3] + 3 [(\text{NH}_4)_2\text{SO}_4]\}}$$

(Stelson & Seinfeld, 1982)

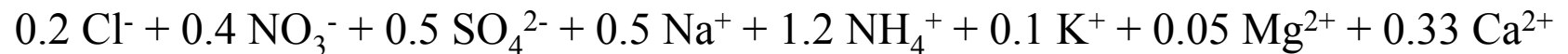
Revisited (→ 3.4.3.1.1): **N(-III) phase distribution in air (T, rh)**

Leipzig, Germany, 1998-99:

Winter (2.5°C, 73% rh)



Summer (18.3°C, 63% rh)



(Lammel et al., 2001)

9. Methodology

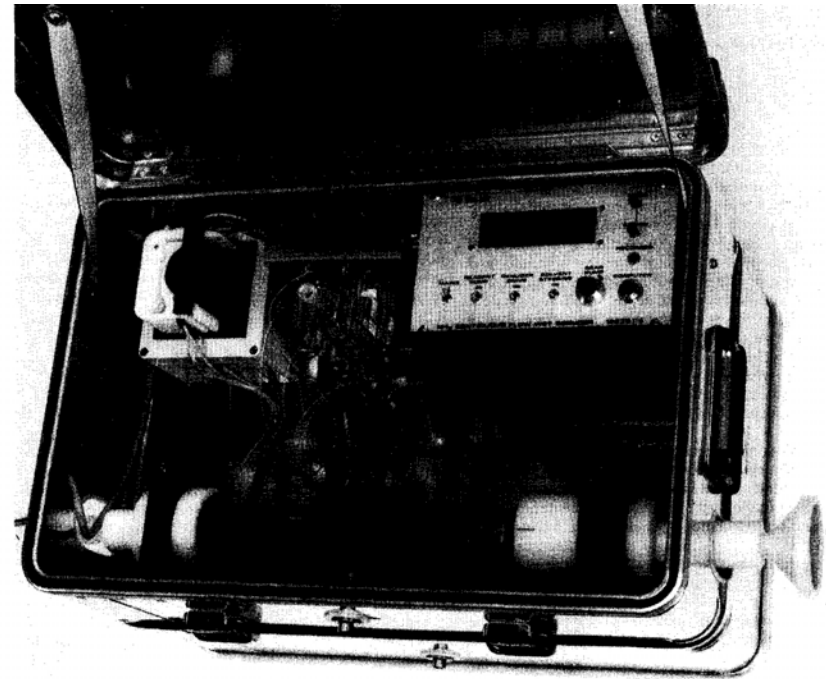
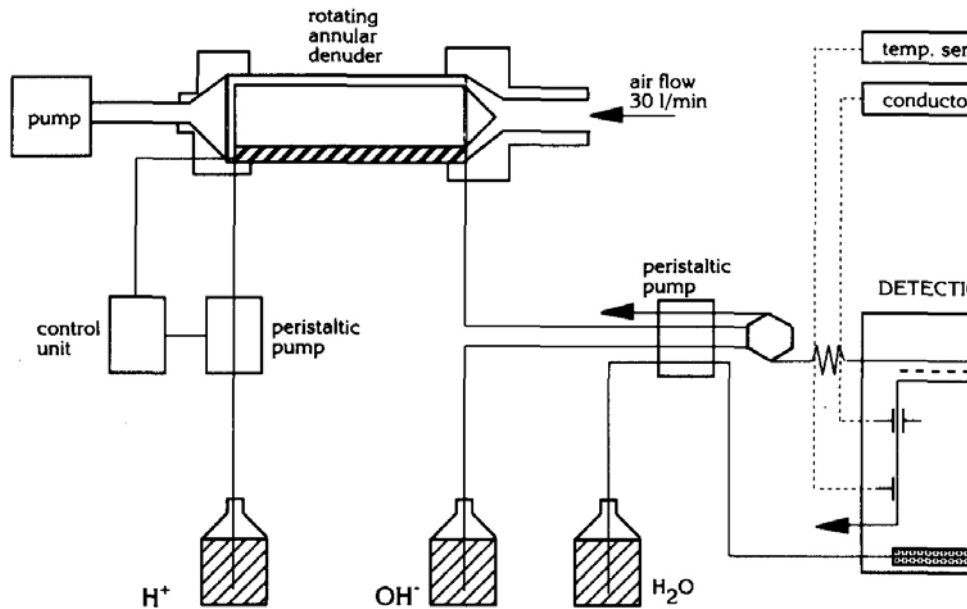
9.1 Sampling methods

9.1.1 Diffusion techniques

9.1.1.1 Denuder

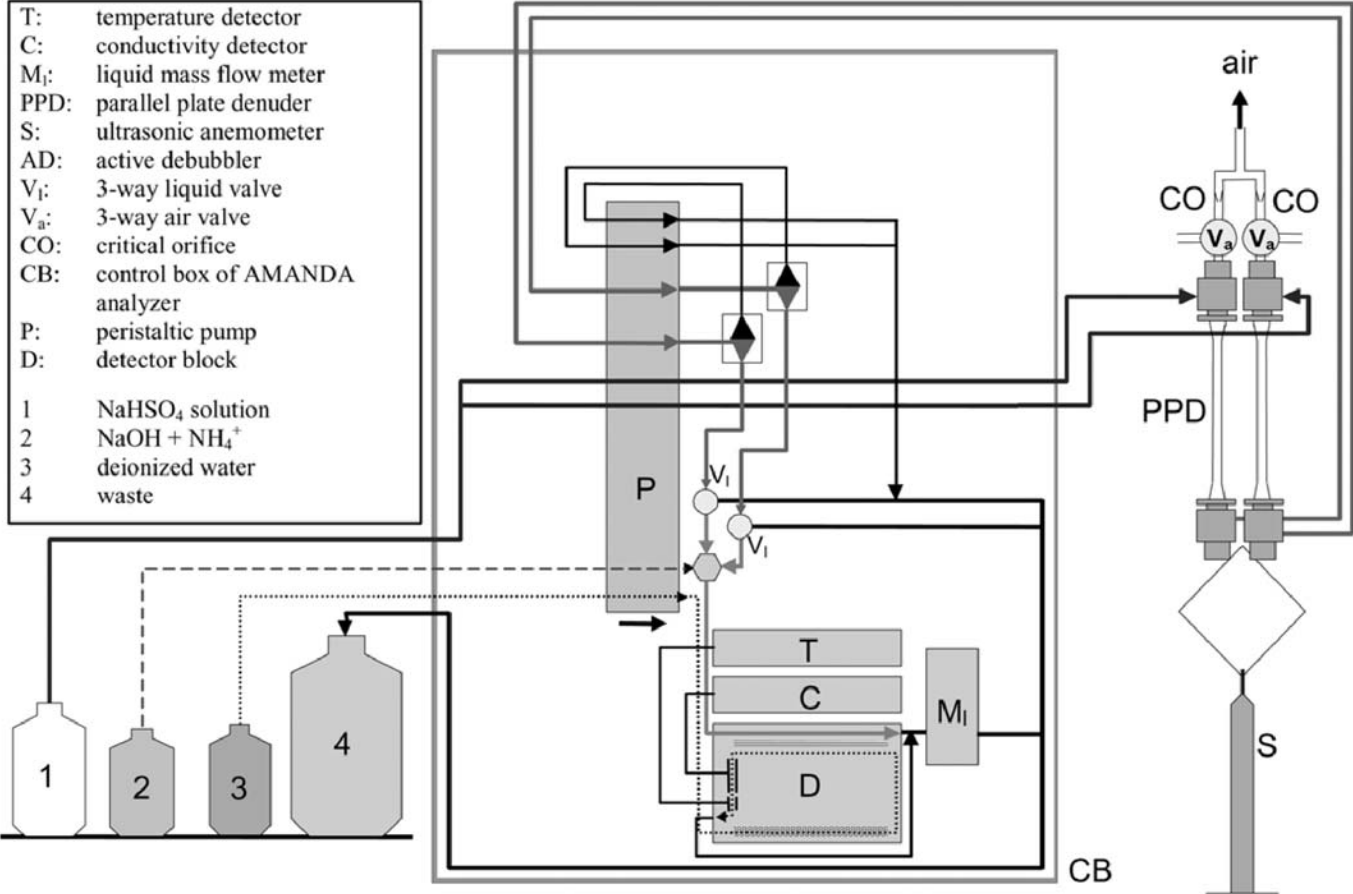
coupled to ion chromatography

- Samples trace gases specifically, chemisorption at wall after diffusion
- Artefact free: particle phase passes without losses
- Rapid automated on-line and (semi-)continuous measurement method



→ Multi-species method (acidic trace gases; e.g. Trebs *et al.*, 2004)

Ammonia measurement by annular denuder sampling with analysis (AMANDA; *Nemitz et al., 2001*): Denuders following *Simon & Dasgupta, 1993*; *Wyers et al., 1993*. Analysis of a counter-flow of $\text{NH}_3(\text{g})$ in deionized water upon removal of $\text{NH}_3(\text{g})$ from the sample flow by high pH at a semipermeable membrane. Control software switches between up- and down-draught channels.



9.1.1.2 Diffusion scrubber

coupled to ion chromatography

- Rapid automated on-line and (semi-) continuous measurement method

(Dasgupta, 1984)

- Wall coating of denuder is replaced by porous tubular membrane wherein a scrubber liquid is continuously flowing
- Liquid stream analysed continuously (e.g. by IC or:

- Flow-injection analyzer + fluorescence detection (Genfa et al., 1989)

Ortho-phthaldialdehyde and sulfite (Na_2SO_3) are added to the sample solution. A

fluorescent product is formed which is detected by a fluorescence detector. Detection limit down to 5 ppt (Junninen et al., 2008; commercial 100 pptv)

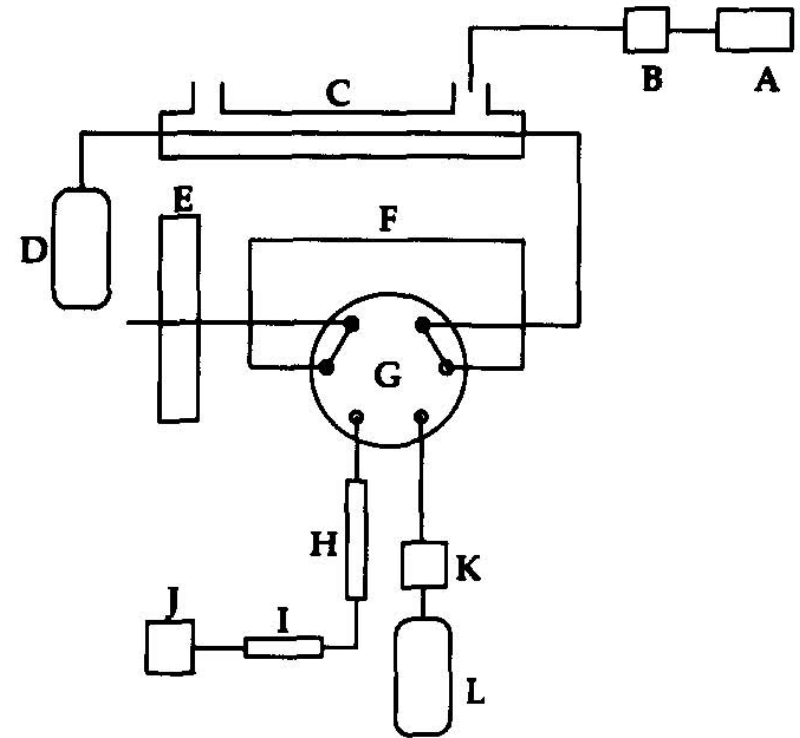


Fig. 1. Schematic diagram of the DS-IC instrument: A, vacuum pump; B, massflow controller; C, diffusion scrubber; D, scrubber liquid reservoir; E, peristaltic pump; F, injection loop; G, injection valve; H, separation column; I, suppressor; J, conductivity detector; K, eluent pump; L, eluent reservoir.

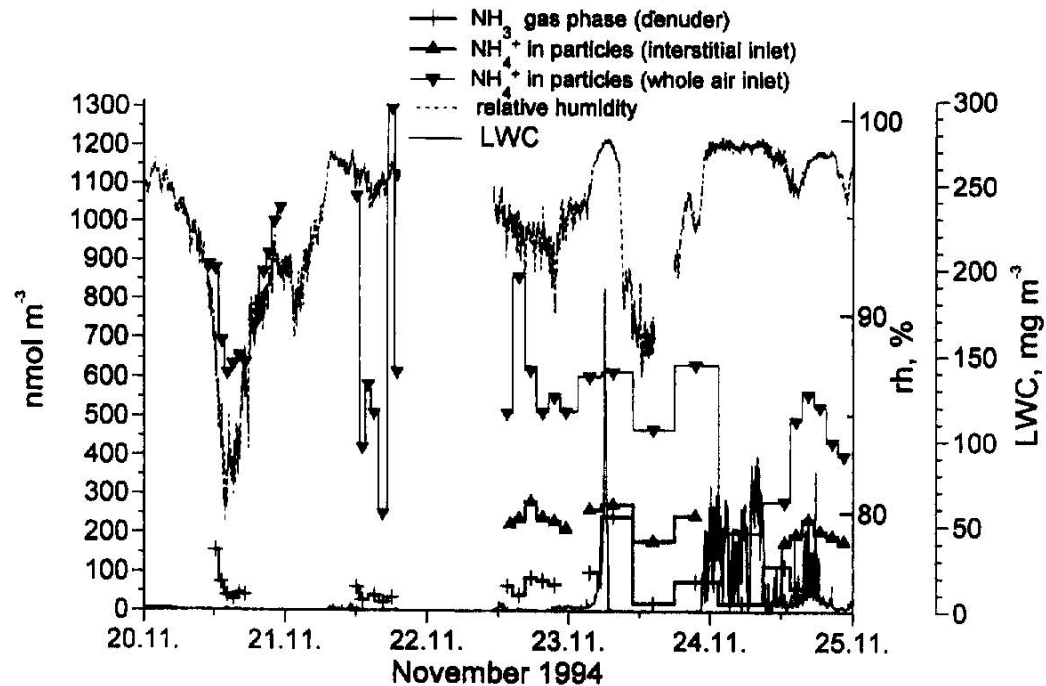
(Lindgren, 1992)

Artefacts of filters:

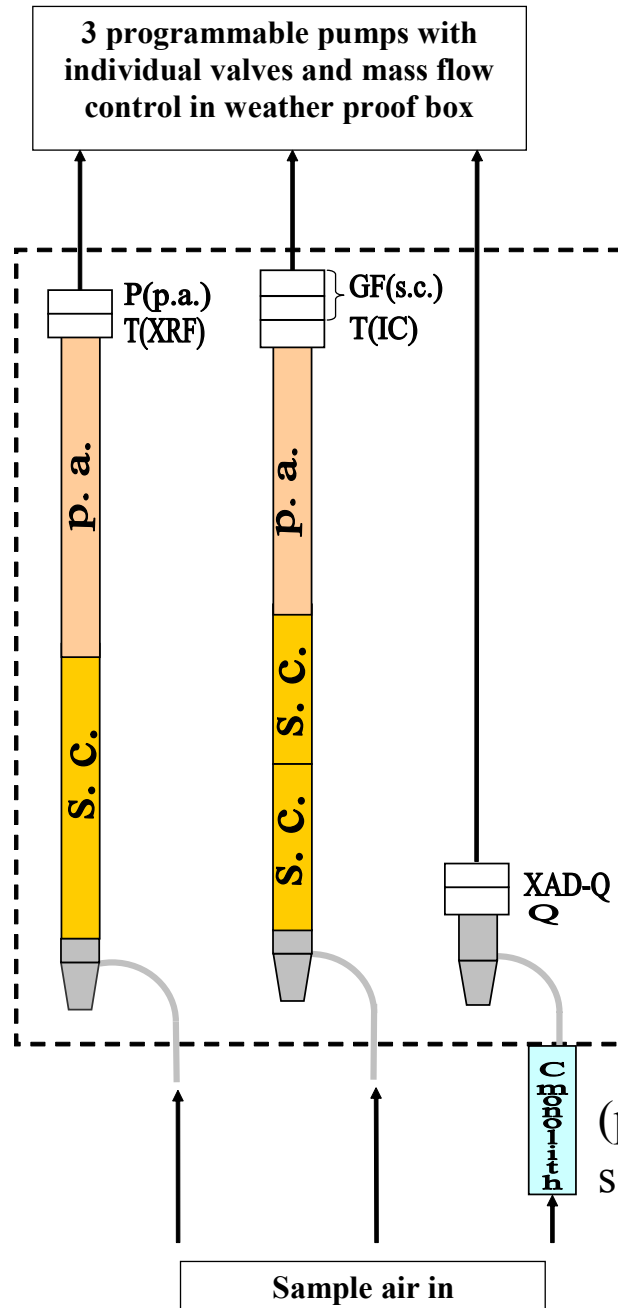
- Underestimate particulate form: semivolatile salts (NH_4Cl , NH_4NO_3) may form and/or volatilize
- Overestimate gaseous form: may adsorb to sampling media

Artefact-free sampling methods:

- Denuder + filterpack: sample gaseous fraction in denuder (first, HCl-coated), sample total on 2 filters, teflon and a gas-adsorbing material (paper or oxalic acid-impregnated paper) downstream
- in fog: denuder + droplet impactor + filter(pack) (*Jaeschke et al., 1998*)



Fine Particle Composition Monitor (PCM)



Reactive Gases

and PM_{2.5} Species

Channel 1:



Channel 2:



Channel 3:

EC, OC, SOC

(p.a. = phosphoric acid,
s.c. = sodium carbonate)

9.1.1.3 Passive sampling

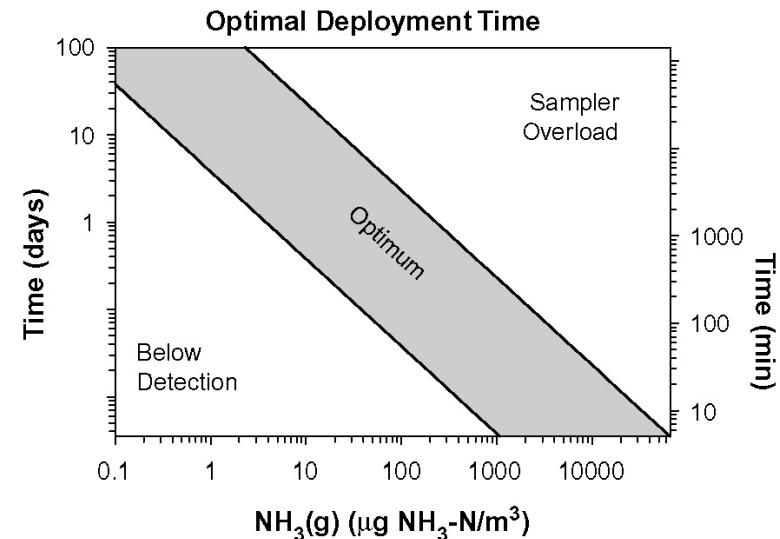
NH₃

Pro / advantages:

- simple, cheap
- no electricity required
- manifold exposure possible (→ high spatial resolution)

Con / disadvantages:

- low temporal resolution
- wind velocity dependence of sampling rate difficult to suppress
- saturation problems (O₃: I⁻, starch, Schönbein)



Citric acid impregnated filter membranes to adsorb alkaline substances, hence NH_3

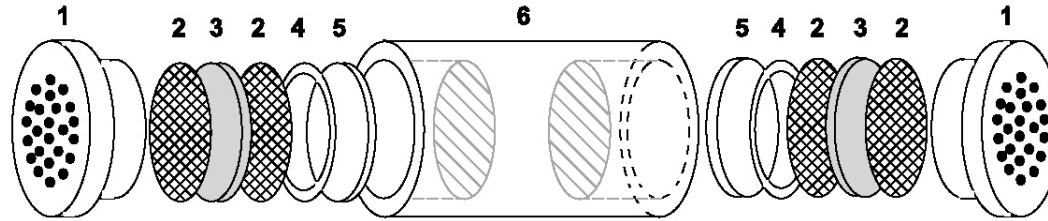
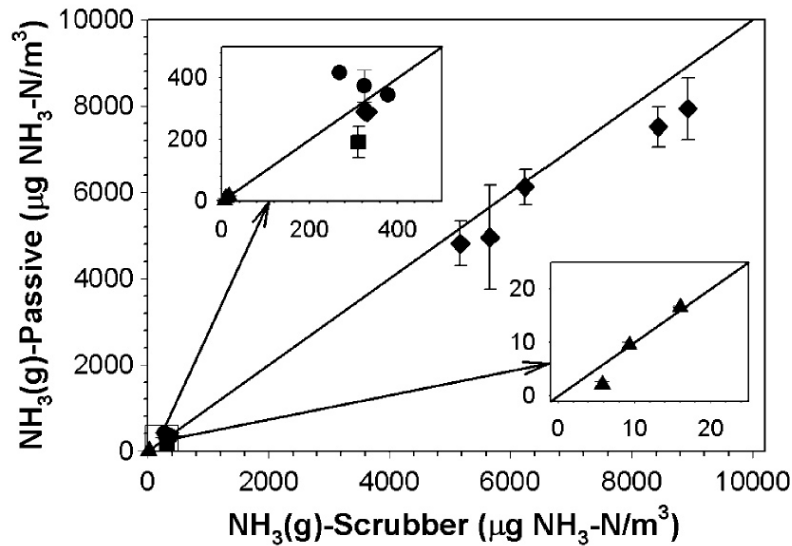


Fig. 1. Components of the Ogawa Passive Sampler. The sampler body (6) is 2 cm (outer diameter) \times 3 cm (length) and has two independent cavities (1.4 cm inner diameter) each containing a diffusive-barrier end-cap (1), a reactive filter (3) between an inner and outer stainless steel screen (2), and a retainer ring (4) over a base pad (5). See ogawausa.com for additional design and deployment details.



Calibration against trapping in aqueous solution (*Roadman et al., 2003*)

Passive, but wind driven rather than diffusion driven

Sampling proportional to wind velocity:
m wind velocity proportionally accumulated

wind speed weighted flux:

$$F_{hzu} = m/(A\Delta t)$$

indices: horizontal, height-dependency, wind velocity u

cross section A

concentration c:

$$m = Vc = uA\Delta tc$$

$$c = u/F_{hzu}$$

Horizontally oriented denuders:

$$\text{cross section } A = \pi r^2$$

Efficiency factor $K_1 = 0.77$ (flow rate response to wind velocity)

on various heights in order to derive net vertical fluxes

(Schjoerring et al., 1992; Schjoerring, 1995)

Artefact-free sampling methods for the particulate phase:

9.1.2 Particle scrubber

- Rapid automated on-line and (semi-)continuous measurement method
- Addresses particulate phase

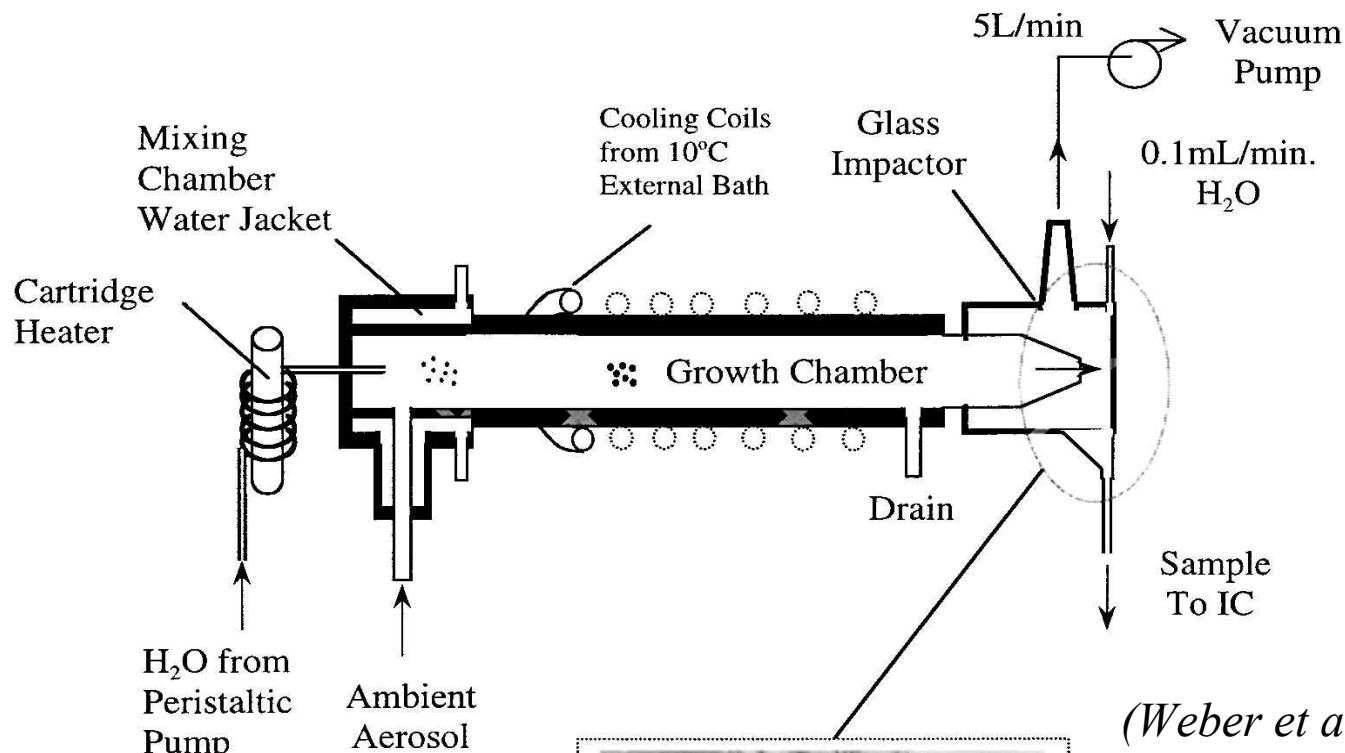
particle scrubber (particles are collected by inertial techniques):

„particle-into-liquid sampler (PILS) (air), liquid stream analysed for cations and anions $0.1 \mu\text{g}/\text{m}^3$

MDL = method detection limit:= the minimum detectable concentration of analyte that a method can reliably detect. Defined as 3x the standard deviation of repeated measurements on a blank sample, σ_b .

(Long & Winefordner, 1983)

Particle growth and removal should be fast enough to minimize NH_3 losses into the droplets (?)

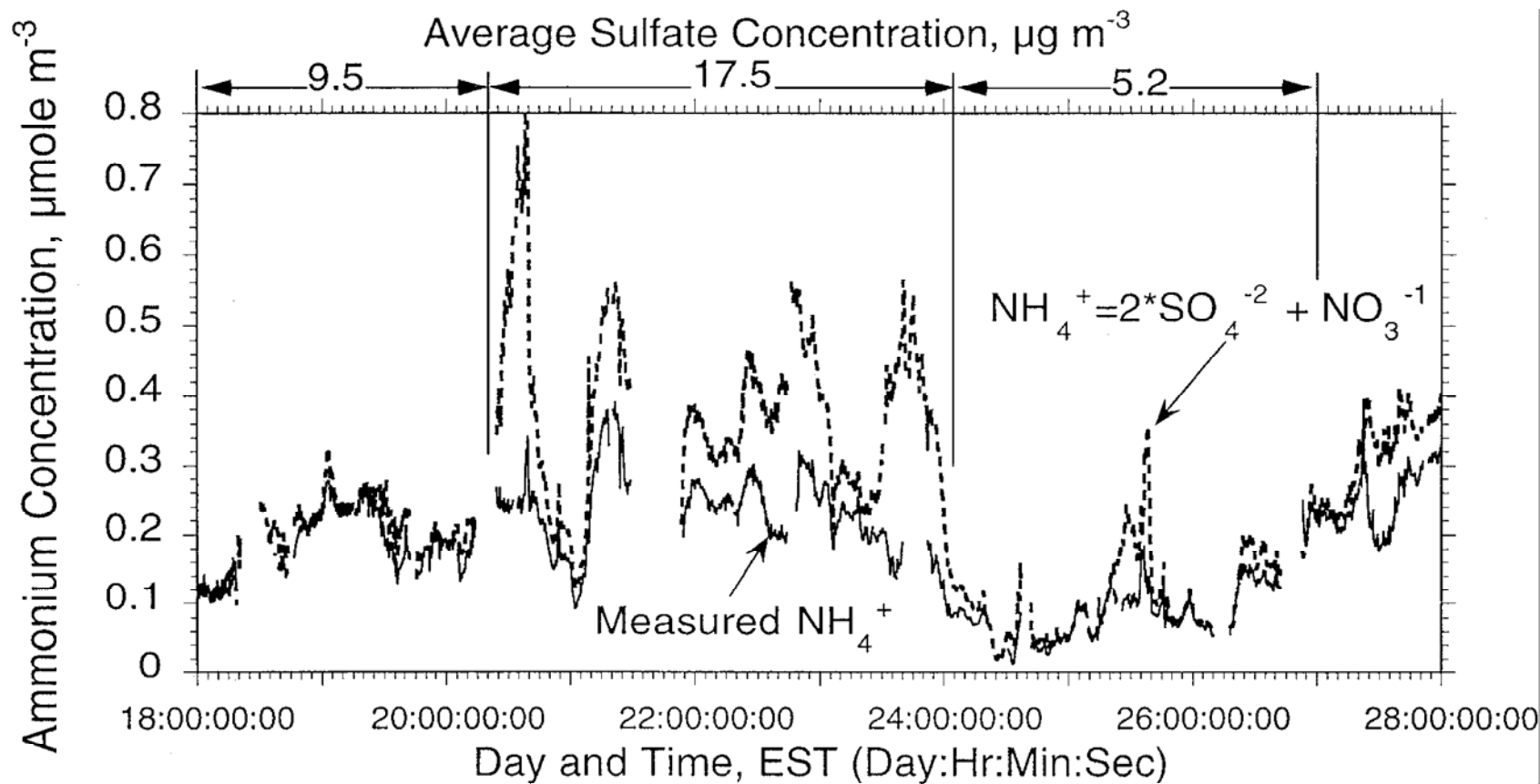


(Weber et al., 2001)

Application

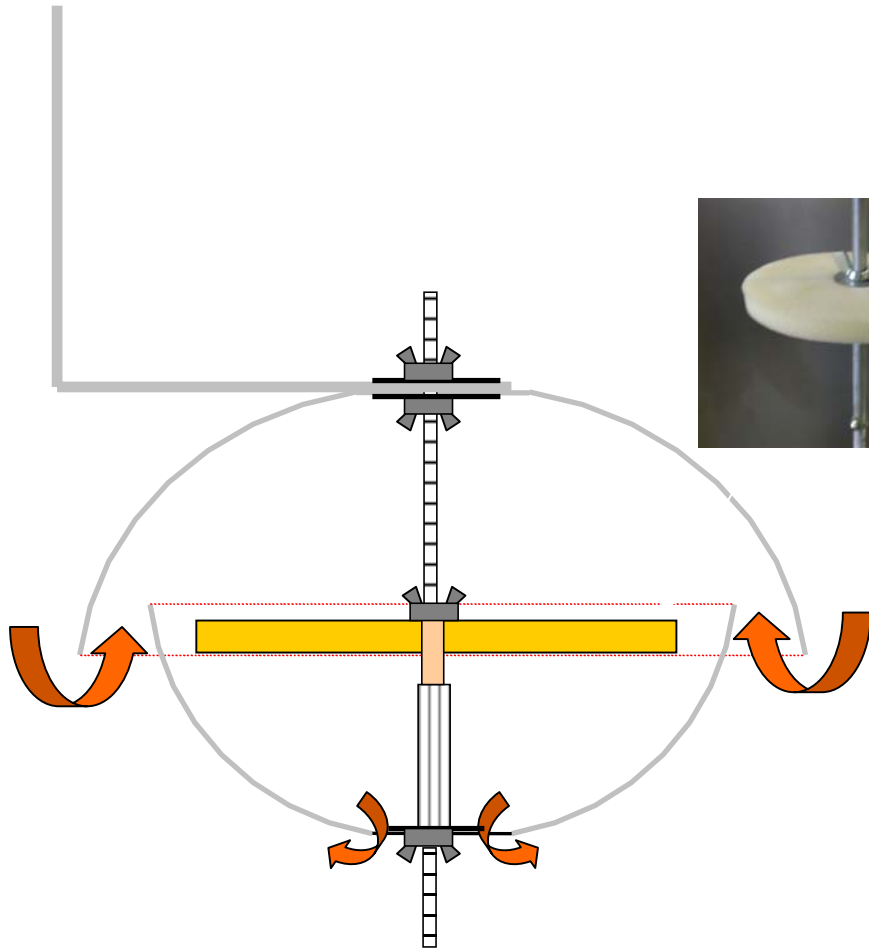
of the particle-into-liquid sampler (PILS):

Time series of temporally high resolved NH_4^+ and $(2 \text{SO}_4^{2-} + \text{NO}_3^-)$



(Weber et al., 2001)

Used for sampling of organics:



- sunlight
- precipitation
- wind effects
- particles

Klánová et al., 2006, 2008

9.2.1 Trace substance measurement after sampling

9.2.1.1 Ion chromatography

Here: Cation chromatography,

two column technique (electrolyte in eluent: H^+/Cl^- , sample components NH_4^+ , A^+),

suppression electrolyte: tertiary butylammonium hydroxide, $(t\text{-C}_4\text{H}_9)_4\text{N}^+\text{OH}^-$:

Reactions in separator column (weak cation exchanger):



Instrument detection limit IDL:= smallest signal above background noise that can be detected by an instrument based on laboratory blanks (standards) $\approx 50 \mu\text{g/L}$ for NH_4^+ by IC.

Reactions in separator column (Keith et al., 1983; Long & Winefordner, 1983)

H^+

A^+ MDL of combined sampling and analysis method [$\mu\text{g}/\text{m}^3$]:

$$\text{NH}_4^+ \text{ MDL} = 0.05 \times 10^{-6} f_d V_{\text{inj}}[\text{mL}] / V_{\text{air}}[\text{m}^3] + 3\sigma_b[\mu\text{g}/\text{m}^3]$$

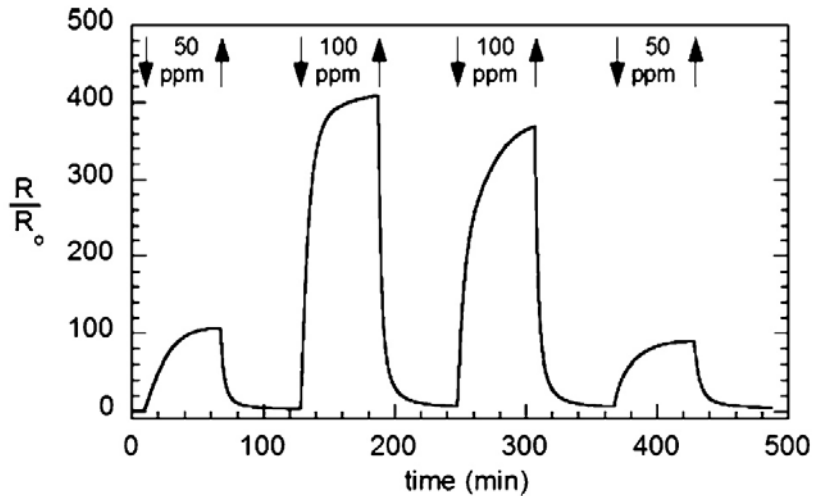
$$V_{\text{air}}[\text{m}^3] = F_{\text{air}}[\text{m}^3/\text{h}] \Delta t[\text{h}]$$

with:

dilution factor (injected volume/stripped volume) f_d , injected and sampled volumina V_{inj} , V_{air} , sampling time Δt , sample air flux F_{air} , standard deviation of repeated measurements on a blank sample, σ_b .

Ammonia methods: Conductivity sensor

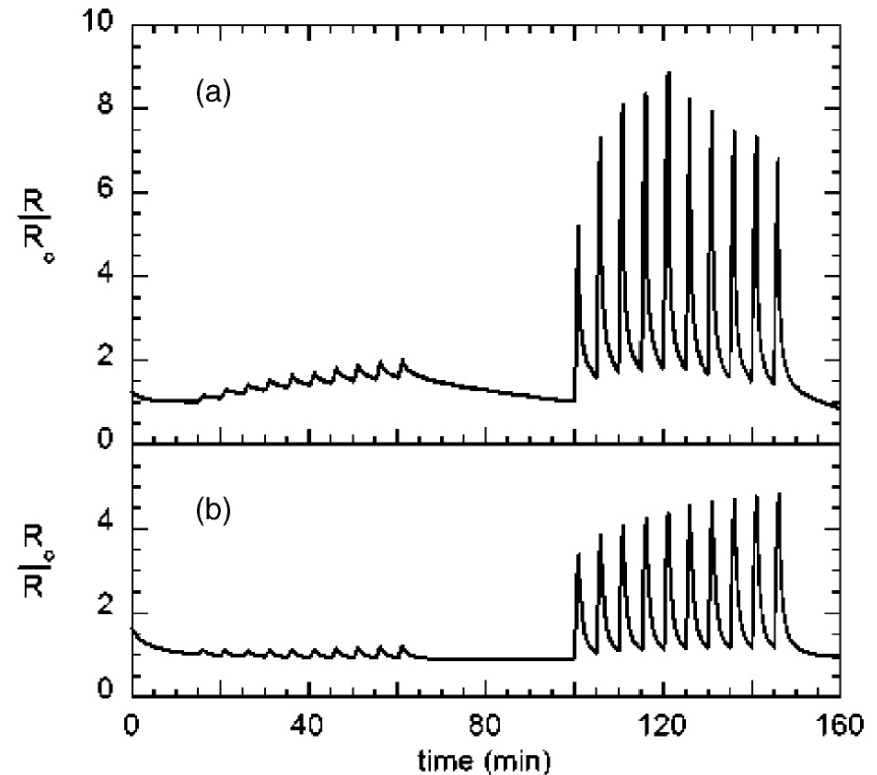
Mobility of Ag^+ in AgBr layer sensitive to e.g. $(\text{CN})_2$, NH_3 (\rightarrow as $\text{Ag}(\text{NH}_3)_2^+$)
 \rightarrow NH_3 determination by Cu^+ ion mobility reduction as $\text{Cu}(\text{NH}_3)_2^+$ in CuBr film,
constant voltage, electrometer



Calibration: 50, 100, 1 and 5 ppm NH_3 .

(a) CuBr, (b) SnO_2 (commercial)

(Lauque et al., 2004)



Ammonia methods: other

- Tunable diode laser absorption spectrometry (TDLAS): d.l. ≈ 0.1 ppbv (e.g. *Li et al., 2006*)
- Near-IR photoacoustic spectroscopy: d.l. ≈ 5 ppbv, interference of CO_2 , H_2O corresponding to 36 and 100 ppbv NH_3 , respectively (*Besson et al., 2006*)
- Chemical ionisation mass spectrometry (CI-MS; ionisation by chemical reaction): rapid, well suited for airborne measurements (*Huey et al., 2007*)

Revisited (\rightarrow 0.2.3):

$$\text{Molar concentration } c_{\text{NH}_3}[\text{nmol/m}^3] = 10^3 c_{\text{NH}_3}[\mu\text{g/m}^3] / M_{\text{g NH}_3}[\text{g/mol}] = m_{\text{NH}_3}/V_{\text{air}}$$

$$\begin{aligned} \text{Volume mixing ratio } \mu_{\text{V NH}_3} &= V_{\text{NH}_3}/V_{\text{air}} [\text{ppbv}] = V_{\text{NH}_3}[\mu\text{L}]/V_{\text{air}}[\text{m}^3] = \\ &= 10^{-12} c_{\text{NH}_3}[\text{nmol/m}^3] V_{\text{M}}[\text{L/mol}] \end{aligned}$$

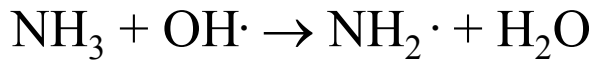
With:

molar mass $M_{\text{g NH}_3} \approx 17$ g/mol

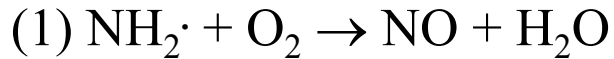
molar volume at $T_0=273$ K and $p_0=101325$ Pa: $V_{\text{M}} = 22.414$ L/mol

$$\mu_{\text{V NH}_3} = 1.32 \text{ ppbv per } \mu\text{g/m}^3$$

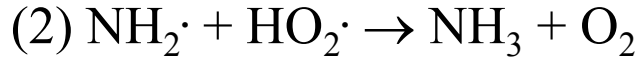
5.1.2 Gas-phase chemistry



$$k = 0.16 \times 10^{-12} \text{ cm}^3/\text{molec}/\text{s}$$



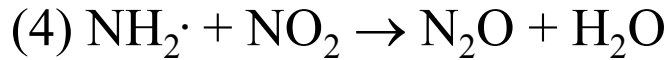
$$k_1 < 6 \times 10^{-21} \text{ cm}^3/\text{molec}/\text{s}$$



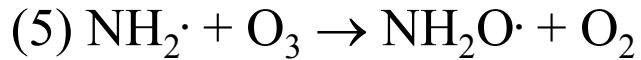
$$k_2 = 34 \times 10^{-12} \text{ cm}^3/\text{molec}/\text{s}$$



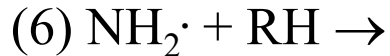
$$k_3 = 17 \times 10^{-12} \text{ cm}^3/\text{molec}/\text{s}$$



$$k_4 = 19 \times 10^{-12} \text{ cm}^3/\text{molec}/\text{s}$$



$$k_5 = 0.16 \times 10^{-12} \text{ cm}^3/\text{molec}/\text{s}$$



too slow to be of any significance

$$-\text{dc}_{\text{NH}_3}/\text{dt} = k_{\text{OH}}^{(1)} c_{\text{NH}_3} = k_{\text{OH}}^{(2)} c_{\text{OH}} c_{\text{NH}_3}; \tau_{\text{OH}} = (k_{\text{OH}}^{(1)})^{-1}$$

≈ 3 months for the global annual tropospheric mean (1.16×10^6 OH/cm³)

≈ 10 days inner tropics near ground ($\approx 10^7$ OH/cm³; *Spivakovsky et al., 2000*)

$$-\text{dc}_{\text{NH}_3}/\text{dt} = k_{\text{OH}}^{(1)} c_{\text{NH}_3} + k_{\text{dep}}^{(1)} c_{\text{NH}_3}$$

$$\tau_{\text{air}} = (k_{\text{OH}}^{(1)} + k_{\text{dep}}^{(1)})^{-1}$$

Wet deposition

Revisited (→ 4.3.1):

Simplified rate (pseudo-1st order):

$$-dc_i/dt = k_{\text{wet dep}}^{(1)} c_i; \tau_{\text{wet dep}} = (k_{\text{wet dep}}^{(1)})^{-1}$$

$$\tau_{\text{wet dep}} = [(1-\theta) \varepsilon_{\text{gas}} r + \theta \varepsilon_{\text{part}} r]^{-1}$$

r = rain repetition rate, below cloud, in cloud (s^{-1}), ε = scavenging coefficient
(dependent on Henry coefficient K_H , particle size D , type of precipitation)

$$\text{Trace gases: } k_{\text{wet dep}}^{(1)} = R E e^{-z/Z_i} / [Z_i (1/K_H R T_Z + L_V)]$$

with: R = annual rain rate (e.g. $1\text{m/a} = 3.2 \times 10^{-8} \text{ m/s}$),
 $E = 1.33$ = enhancement factor (evaporation, collecting),
 z = characteristic height in which cloud forms (e.g. Stratus: 3.5 km),
 $Z_i \approx 2.2 \text{ km}$ = scale height of i (no fast chemical sinks, else lower)
 K_H = Henry [M/bar],
 T_Z = temperature at scale height of i ,
 L_V = liquid water volume fraction (e.g. 10^{-6})

(Brimblecombe & Dawson, 1984)

In-cloud and below-cloud scavenging

Revisited (→ 3.3.3.1): Dissolution of gases - thermodynamic equilibrium

...with diluted solutions (ideal behaviour).

The scavenging efficiency of gaseous molecules is dependent on water solubility:

$$\begin{aligned}\varepsilon_{i(g) \text{ sol}} &= n_{(\text{sol})} / (n_{(\text{sol})} + n_{(\text{g})}) = n_{(\text{sol})} / [n_{(\text{sol})} + p_i V_{\text{air}} / (R_g T)] = \\ &= n_{(\text{sol})} / [n_{(\text{sol})} + H_i n_{(\text{sol})} V_{\text{air}} / (R_g T n_{\text{H}_2\text{O}})] = \\ &= [1 + H_i M_w / (R_g T L)]^{-1}\end{aligned}$$

with: Henry coefficient H_i [atm] = $p_i/x_i = p_i/(c_i/10^3/M_w)$,

liquid water content L [g/m³]

solubility $s(T) = s(T_0) * \exp[-\Delta H_{\text{sol}}/R * (1/T-1/T_0)]$

gas constant R_g , M_w [g/mol], 10^3 [cm³/L],

(Warneck, 1986)

H from another Henry coefficient:

$$H = (10^3/M_w) * \rho_{\text{H}_2\text{O}}/K_H \text{ [M bar}^{-1}\text{]}$$

$$K_H \text{ [M bar}^{-1}\text{]} = 10^2 s/M_w p = (10^3/M_w) * \rho_{\text{H}_2\text{O}}/H$$

s [mg/L]

Transfer from gas to aqueous phase treated like a chemical reaction (‘pseudo-reaction’):

$$dc_{i \text{ aqu}}/dt = k_{\text{mt}} (c_{i \text{ (g)}} - c_{i \text{ aqu}}/RTK_{\text{H}}^*)$$

with mass transfer rate coefficient $k_{\text{mt}} = (\sum_i \tau_i)^{-1}$

- Slightly soluble gases (i.e. $RTK_{\text{H}} < 750$): Henry’s law equilibrium rapidly established at the drop surface, transport rate limiting is diffusion within the drop: $k_{\text{mt}} \approx \tau_{\text{da}} = r^2/(\pi^2 D_{\text{a}})$
- Soluble gases (i.e. $RTK_{\text{H}} > 750$): Henry’s law equilibrium establishment limited by diffusion in the gas-phase and by transport through the interface: $k_{\text{mt}} \approx \tau_{\text{da}} = [r^2/(3D_{\text{g}}) + 4r/(3\alpha\langle v \rangle)]^{-1}$

Revisited (→ 1.5.2.2):

Deviation from phase equilibrium due to kinetic limitations - mass transport considerations

Transfer from gas to aqueous phase treated like a chemical reaction (,pseudo-reaction‘):

$$dc_{i \text{ aqu}}/dt = k_{\text{mt}} (c_{i \text{ (g)}} - c_{i \text{ aqu}}/RTK_{\text{H}}^*)$$

Table 3 Henry's law partition coefficients K_{H}^{\ominus} at $T = 298 \text{ K}$, heats of vaporization ΔH_{soln} divided by the gas constant R_{g} , mass accommodation coefficients α , transfer coefficients k_t , and the associated time constants for the approach to Henry's law equilibrium

Constituent	K_{H}^{\ominus} ^a /mol dm ⁻³ atm ⁻¹	($\Delta H_{\text{soln}}/R_{\text{g}}$) /K	$R_{\text{g}}TK_{\text{H}}$	α ^b	k_t ^c /s ⁻¹	τ_{H} ^d /s	Ref. ^e
O ₂	1.3×10^{-3}	1500	3.8×10^{-2}	0.01*	5.3×10^2	8.9×10^{-8}	19
O ₃	1.1×10^{-2}	2300	3.7×10^{-1}	0.004	5.3×10^2	2.1×10^{-6}	20
OH	3.0×10^1	4500	1.9×10^3	0.004	3.5×10^5	3.9×10^{-3}	21
HO ₂	4.0×10^3	5900	2.3×10^5	0.01	4.2×10^5	8.2×10^{-1}	21
H ₂ O ₂	1.0×10^5	6300	6.1×10^6	0.11	1.0×10^6	5.9	22
CH ₃ OOH	3.0×10^2	5300	1.6×10^4	0.004	1.8×10^5	4.5×10^{-2}	22
CH ₃ OO	6.0	–	1.4×10^2	0.01*	5.3×10^2	4.0×10^{-4}	23
CH ₃ OH	2.2×10^2	4900	1.1×10^4	0.02	6.4×10^5	1.7×10^{-2}	24
HCHO	3.0×10^3	7200	2.1×10^5	0.01*	4.4×10^5	4.8×10^{-1}	25
HCOOH	5.5×10^3	5700	3.1×10^5	0.013	4.6×10^5	4.5	26
CO ₂	3.4×10^{-2}	2400	1.1	2×10^{-4}	5.3×10^2	1.1×10^{-4}	10
NO	1.9×10^{-3}	1500	5.6×10^{-2}	0.02*	5.3×10^2	8.4×10^{-8}	27
NO ₂	7.0×10^{-3}	2500	2.4×10^{-1}	0.001*	5.3×10^2	2.1×10^{-6}	28
NO ₃	2.0	2000	6.4×10^1	0.003	5.3×10^2	3.4×10^{-4}	29
N ₂ O ₅	∞	–	–	0.02	3.5×10^5	–	–
HNO ₂	5.0×10^1	4900	2.5×10^3	0.05	7.5×10^5	5.0×10^{-2}	30
HNO ₃	$2.4 \times 10^6/K_{\text{d}}$	8700	1.5×10^7	0.05	6.5×10^5	2.8×10^2	31
HOONO ₂	1.4×10^4	–	3.2×10^5	0.01*	2.7×10^5	1.6	32
NH ₃	6.1×10^1	4200	2.7×10^3	0.09	1.4×10^6	2.8×10^2	33
SO ₂	1.2	3200	4.6×10^1	0.1	7.5×10^5	4.3×10^{-2}	34
SO ₃	∞	–	–	0.01*	2.7×10^5	–	–

^a 1 atm = $1.01325 \times 10^5 \text{ Pa}$. ^b Mass accommodation coefficients are from Warneck *et al.*¹² except for OH and HO₂ from Hanson *et al.*,²¹ for CH₃OOH, CH₃OH and HNO₃ from Davidovits *et al.*,³⁵ and for NO₃ from Thomas *et al.*²⁹ Asterisks indicate estimates. ^c Transfer coefficients for O₂, O₃, CH₃OO, CH₃OH, CO₂, NO, NO₂ and NO₃ are determined by molecular diffusion in the aqueous phase. ^d Modified Henry's law coefficients were used in calculating τ_{H} (pH 4.5). ^e References for Henry's law coefficients.

(Warneck, 1999)

Revisited (→ 3.4.1):

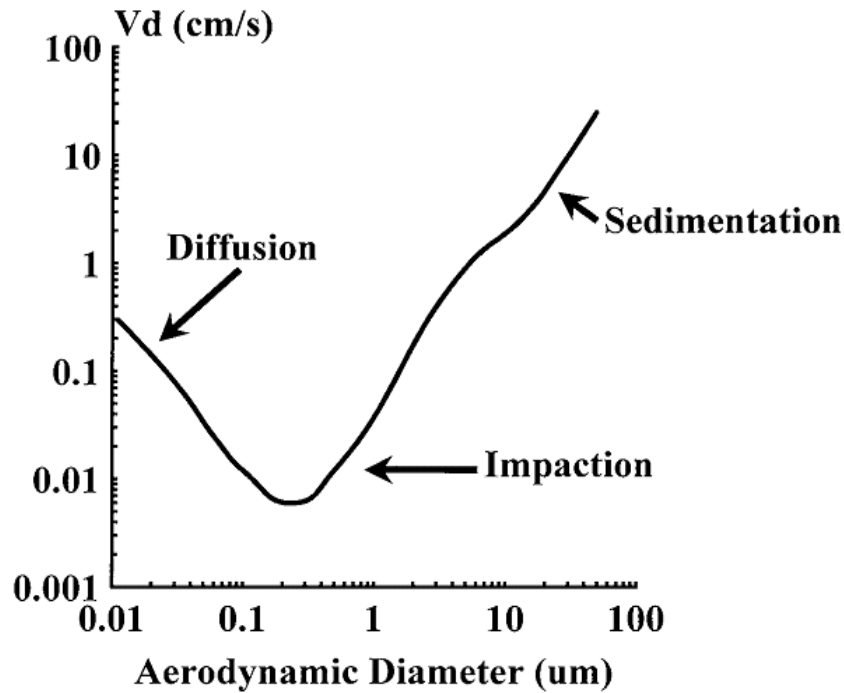
Aerosol particle removal processes

-size dependent residence time; empirical expression:

$$\tau_{\text{dry}} = f(D) = \beta / [(D/0.6)^2 + (D/0.6)^{-2}]$$

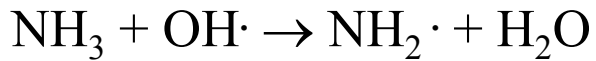
D in μm , $\beta = 1.28 \times 10^8 \text{ s}$ (Jaenicke, 1988)

**Deposition Velocity of Particles (Vd)
as a Function of Aerodynamic Diameter**

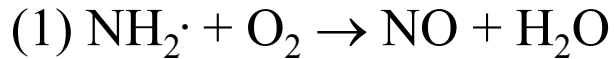


D/2 [μm]	τ [d]	Δs [km]	Δz [m]
0.00 1	0.01	8	20
0.01	1	800	2000
0.1	10	8000	20000
1	10	8000	20000
10	1	800	2000
100	0.01	8	20

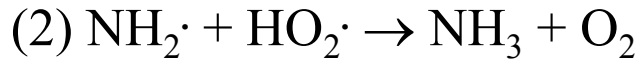
5.1.2 Gas-phase chemistry



$$k = 0.16 \times 10^{-12} \text{ cm}^3/\text{molec}/\text{s}$$



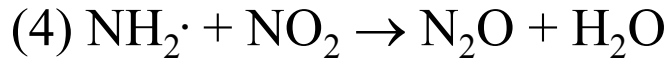
$$k_1 < 6 \times 10^{-21} \text{ cm}^3/\text{molec}/\text{s}$$



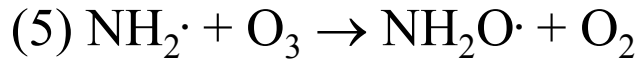
$$k_2 = 34 \times 10^{-12} \text{ cm}^3/\text{molec}/\text{s}$$



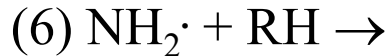
$$k_3 = 17 \times 10^{-12} \text{ cm}^3/\text{molec}/\text{s}$$



$$k_4 = 19 \times 10^{-12} \text{ cm}^3/\text{molec}/\text{s}$$



$$k_5 = 0.16 \times 10^{-12} \text{ cm}^3/\text{molec}/\text{s}$$



too slow to be of any significance

$$-\text{dc}_{\text{NH}_3}/\text{dt} = k_{\text{OH}}^{(1)} c_{\text{NH}_3} = k_{\text{OH}}^{(2)} c_{\text{OH}} c_{\text{NH}_3}; \tau_{\text{OH}} = (k_{\text{OH}}^{(1)})^{-1} \approx 3 \text{ months } (10^6 \text{ OH}/\text{cm}^3)$$

$$-\text{dc}_{\text{NH}_3}/\text{dt} = k_{\text{OH}}^{(1)} c_{\text{NH}_3} + k_{\text{dep}}^{(1)} c_{\text{NH}_3}$$

$$\tau_{\text{air}} = (k_{\text{OH}}^{(1)} + k_{\text{dep}}^{(1)})^{-1} \approx (k_{\text{dep}}^{(1)})^{-1} < 1 \text{ week (or shorter in precipitation)}$$

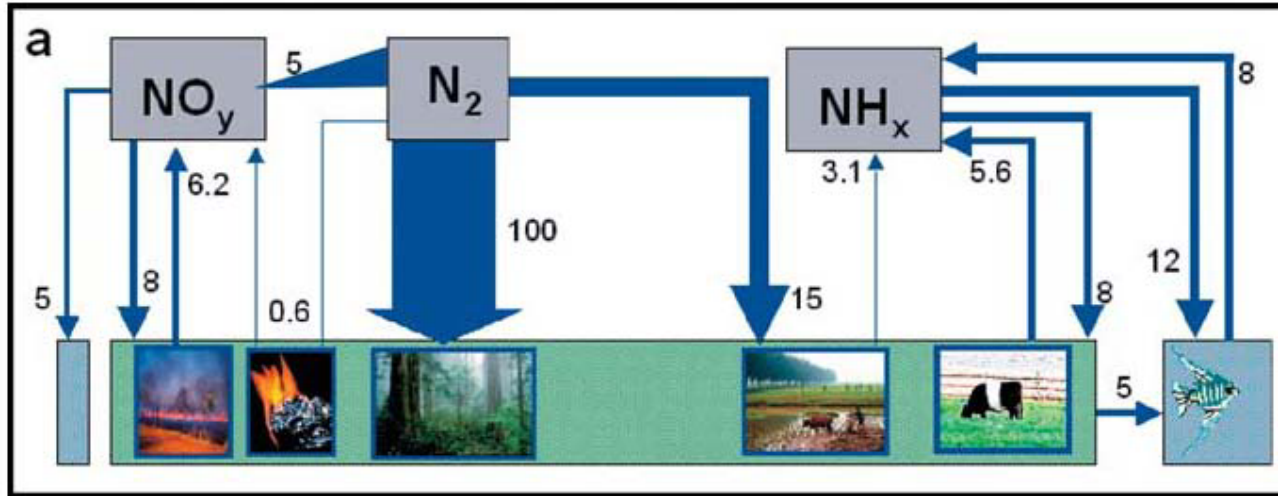
- photochemistry slow, mostly negligible
- rapidly washed out

$$\text{Ammonia budget } dc_{\text{NH}_3}/dt = F_e - k_{\text{OH}}^{(1)} c_{\text{NH}_3} - k_{\text{dep}}^{(1)} c_{\text{NH}_3}$$

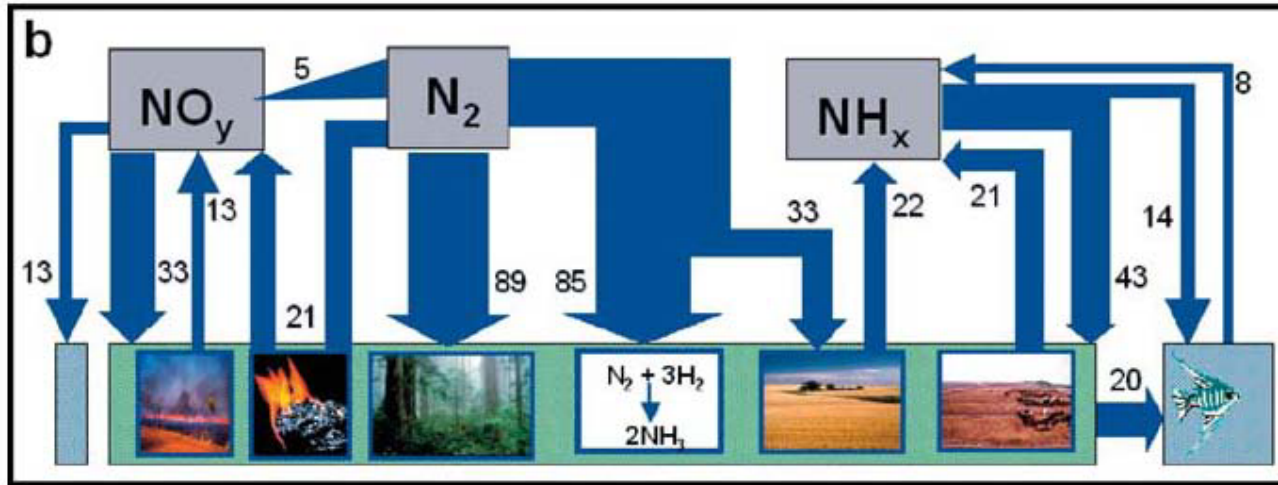
Global N cycle, fluxes (Tg/a)

+80%

1890

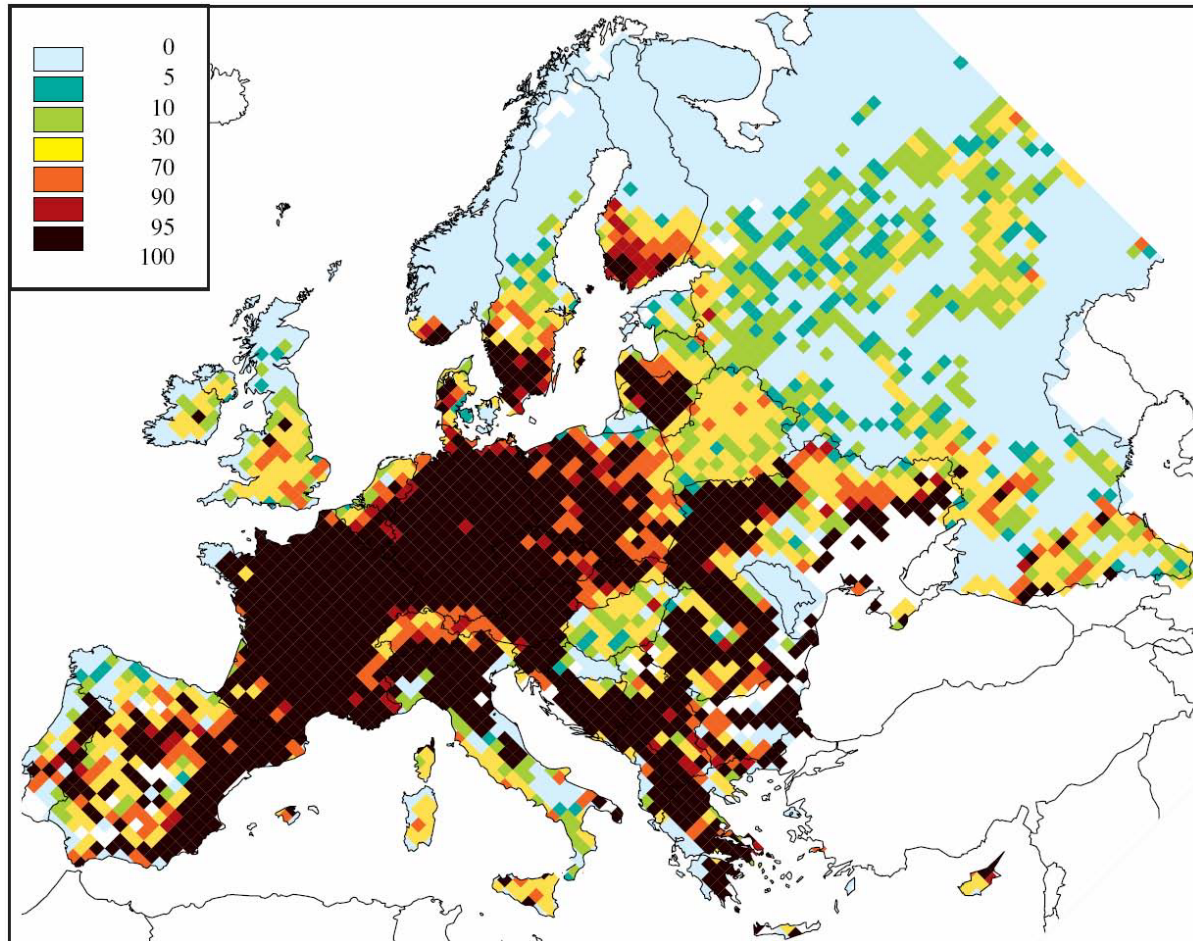


1990



(Hibbard et al., 2006)

Eutrophication: nutrient N



Percentage of total ecosystems area receiving nitrogen deposition above the critical loads for eutrophication for the emissions of the year 2000 (meteorology of 1997)

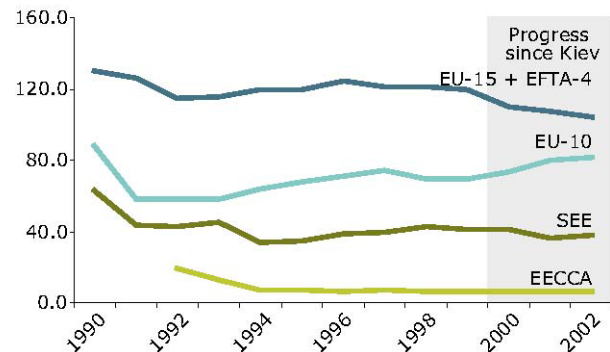
(Sverdrup et al., 1990; *IIASA*)

Ammonia trends Europe

Past emissions in Europe and adjacent seas (Mt/a)

	1980	2004	Δ
NH ₃	7.64	5.74	-25 %
SO ₂	54.3	15.1	-72 %
NO _x	25.7	20.2	-21 %

Mean fertiliser consumption (kg/ha)



Future

EU commitments

EU scenarios

	2000	National Ceilings 2010	Climate Action 2020	Strategy on Air Poll. 2020	Base-line 2030	Climate Action 2030	Climate Action MFR 2030
NO _x	11,581	8,319	5,888	4,657	6,125	5,524	2,849
VOCs	10,654	8,150	5,915	5,251	5,863	5,877	4,101
SO ₂	8,736	6,543	2,806	1,602	2,851	2,371	1,130
			-4%	-28%	-6%		-43%

→ NO₃⁻/SO₄²⁻ and NH₄⁺/(SO₄²⁻ + NO₃⁻) are increasing in depositions

Emission trends (kt) in the EU-25 (EEA, 2006)

5.1.3 Primary particle formation (nucleation)

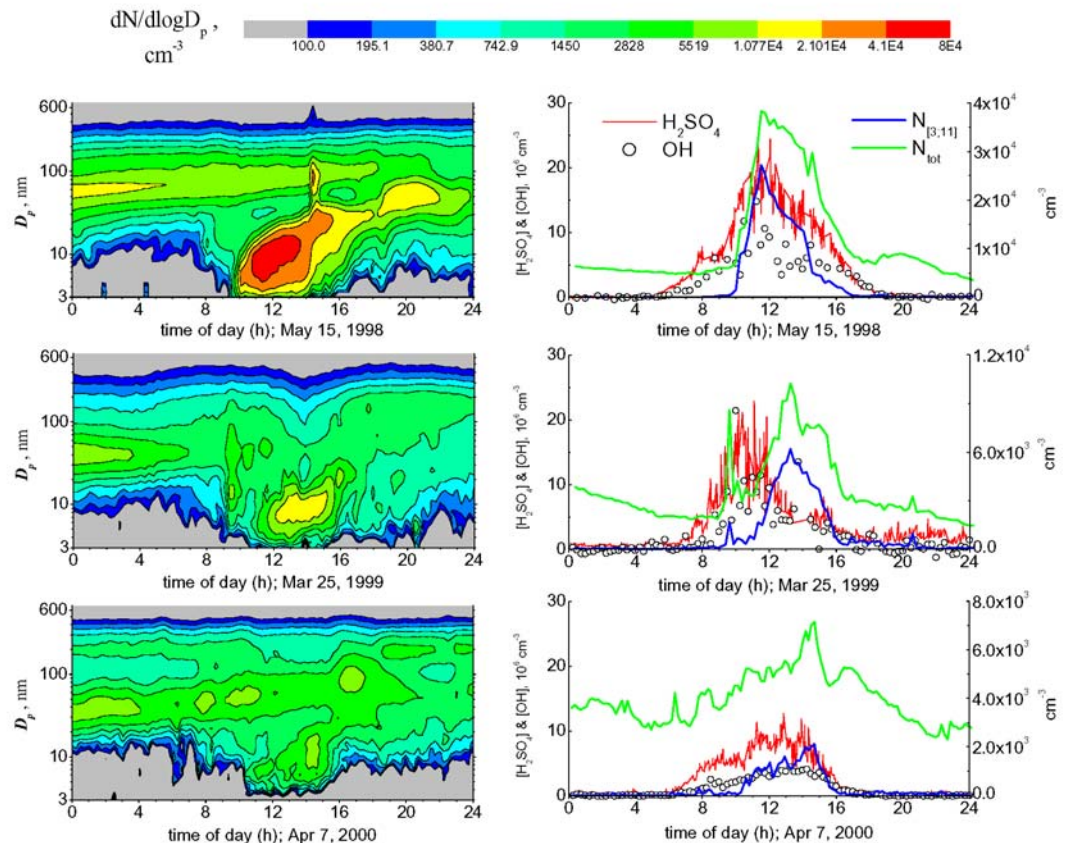
condensational growth



Nucleation events:

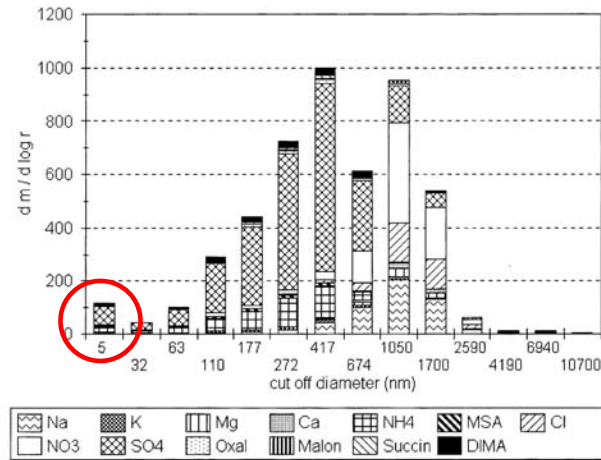
Reasons for occurrence of nucleation events unclear. No simple correlations, key factors unknown. Example: 3 different events on Hohenpeissenberg 1998-2000 (*Birmili et al., 2003*).

The nucleation rate is mostly 2nd order in H_2SO_4 , in general 1st to 2nd. This suggests the prevalence of a bimolecular reaction (collision) of 2 clusters with each one H_2SO_4 molecule for formation of the critical cluster (*Weber et al., 2006*).

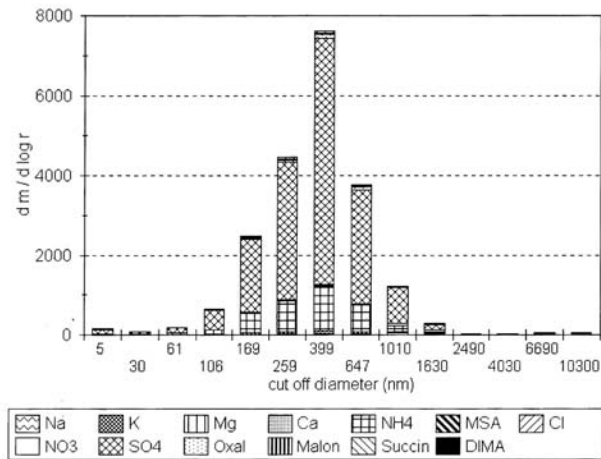


Chemical composition of nucleated particles unknown. What are the smallest particles composed of? E.g. in an urban environment in Mexico (Tecamac), H_2SO_4 accounted for 10% of the 10nm particles.

„Events“ in southern Finland spring 1999:



„Non-events“:

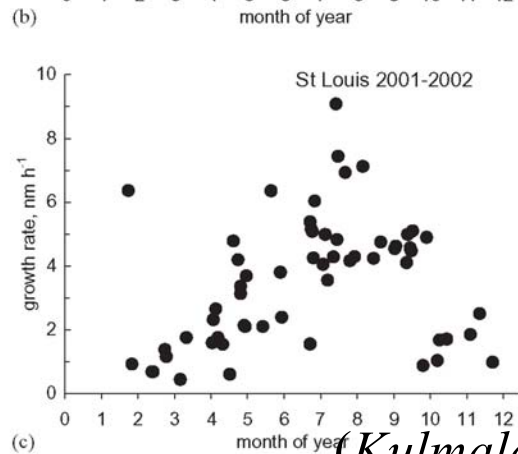
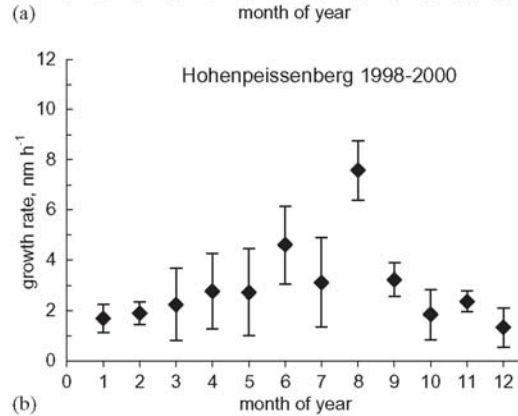
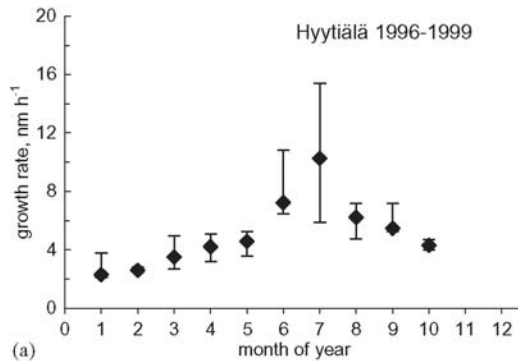


(Mäkelä et al., 2001)

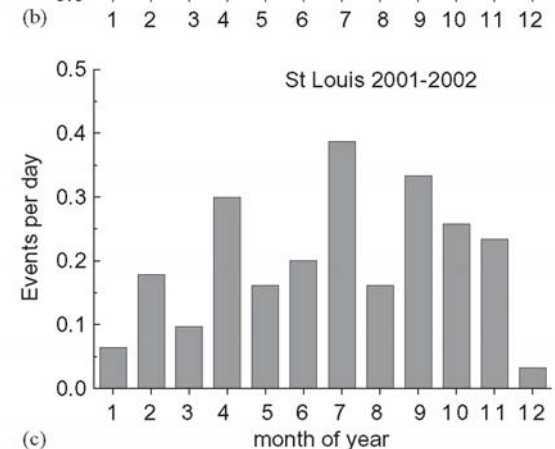
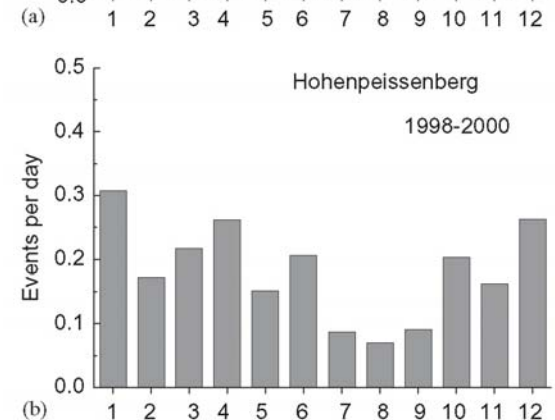
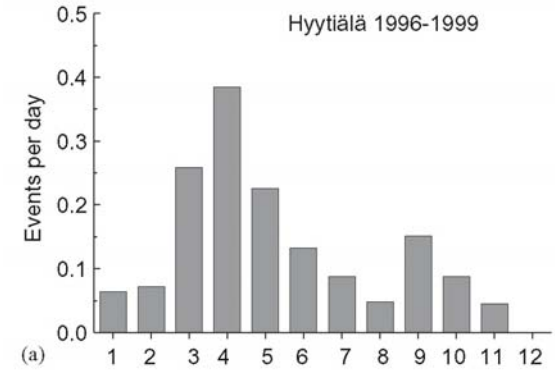
Observed growth rates can often, but also often not be explained by binary nucleation of H_2SO_4 and water (Stolzenburg et al., 2005).

In various environments
growth rates are similar (5-10 nm/h):

seasonalities of particle formation events
do not match:



(Kulmala et al., 2004)



(c)

Critical cluster size ≈ 1 nm.

But smallest particles addressable by state-of-the-art techniques had grown to ≈ 3 nm (n-butanol condensation particle counter) or ≈ 10 nm (analysing by MS).

Hence, nucleation might occur everyday everywhere (measurement gap).

Methodology:

State-of-the-art: Chemical ionization-mass spectrometry (CI-MS) can analyse clusters of ≈ 1000 Da.

Soon: Application of diethylen glycol and oleic acid CPCs counting down to 1.2 nm ≈ 600 Da (*Iida et al., 2008*)

New particle formation (nucleation) mechanisms:

Binary nucleation ($\text{H}_2\text{SO}_4 / \text{H}_2\text{O}$)

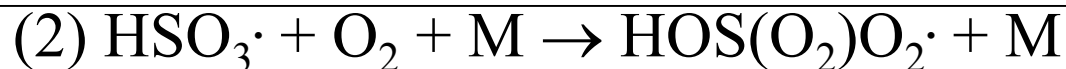
- is too weak and
- has the wrong dependency on $c_{\text{H}_2\text{SO}_4}$ ($\gg 1^{\text{st}}$ order)

Laboratory studies suggest several orders of magnitudes too low nucleation rates, 10^8 - $10^9 \text{ H}_2\text{SO}_4 \text{ cm}^{-3}/1 \text{ particle cm}^{-3} \text{ s}^{-1}$ (,unit J'; *Benson et al., 2008*)

However: 10^3 **higher rates result from in situ-produced rather than evaporated H_2SO_4** (*Berndt et al., 2005, 2006, 2008*).

Possible explanation:

Revisited (\rightarrow 3.3.1):



In these experiments H_2SO_4 was indirectly controlled, however (i.e., not necessarily at the place where it nucleates).

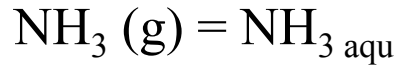
New particle formation (nucleation)

Ternary nucleation ($\text{H}_2\text{SO}_4 / \text{H}_2\text{O} / \text{NH}_3$): Currently accepted as prevailing in the free troposphere and in the marine boundary layer (*Napari et al., 2002*).

In the continental BL indications for possible significance of nucleation of $\text{H}_2\text{SO}_4 / \text{H}_2\text{O} / \text{SOC}$ (*SOC = semivolatile organic compound*). E.g., freshly formed 1.5-2 nm negative particles were much higher concentrated than positive particles of the same size (*Laakso et al., 2007*). For negative clusters, however, no NH_3 association can be expected.

5.1.4 Ammonia air/sea exchange

5.1.4.1 Equilibria

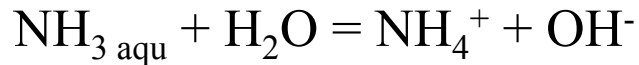


$$\Delta H_{\text{soln}} = +35 \text{ kJ/mol, heat of vaporisation}$$

$$K_{\text{H}} = 6.1 \times 10^{-4} \text{ mol/L/Pa (298 K)}$$

$$K_{\text{H NH}_3} = c_{\text{NH}_3 \text{ aqu}} / p \quad [\text{M/Pa}]$$

$$K_{\text{H NH}_3}^* = (c_{\text{NH}_3 \text{ aqu}} + c_{\text{NH}_4^+}) / p \quad [\text{M/Pa}]$$

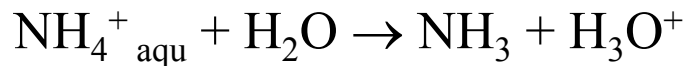


$$K_{\text{B NH}_3} = (c_{\text{NH}_4^+} c_{\text{OH}^-}) / c_{\text{NH}_3 \text{ aqu}} = 1.8 \times 10^{-5} \text{ M}$$

(298 K; $\text{p}K_{\text{B}} = 4.75$)

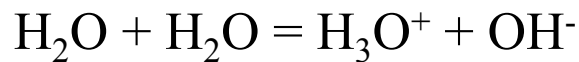
with: $c_{\text{NH}_4^+} / p = K_{\text{H NH}_3} K_{\text{B}} / c_{\text{OH}^-}$

$$\rightarrow K_{\text{H NH}_3}^* = K_{\text{H NH}_3} (1 + K_{\text{B}} / c_{\text{OH}^-})$$



$$K_{\text{A NH}_4^+} = (c_{\text{NH}_3} c_{\text{H}_3\text{O}^+}) / c_{\text{NH}_4^+ \text{ aqu}} = 5.6 \times 10^{-10}$$

(298 K; $\text{p}K_{\text{A}} = 9.25$)

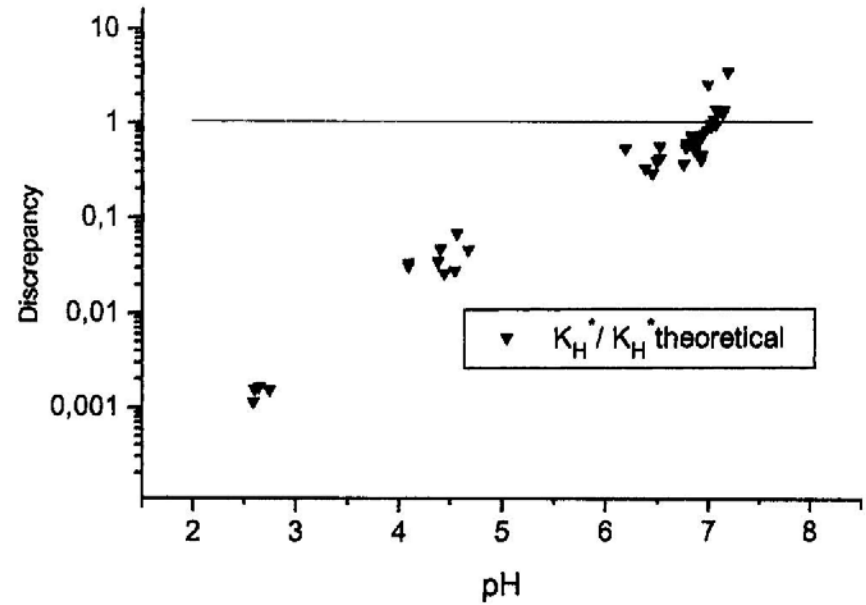
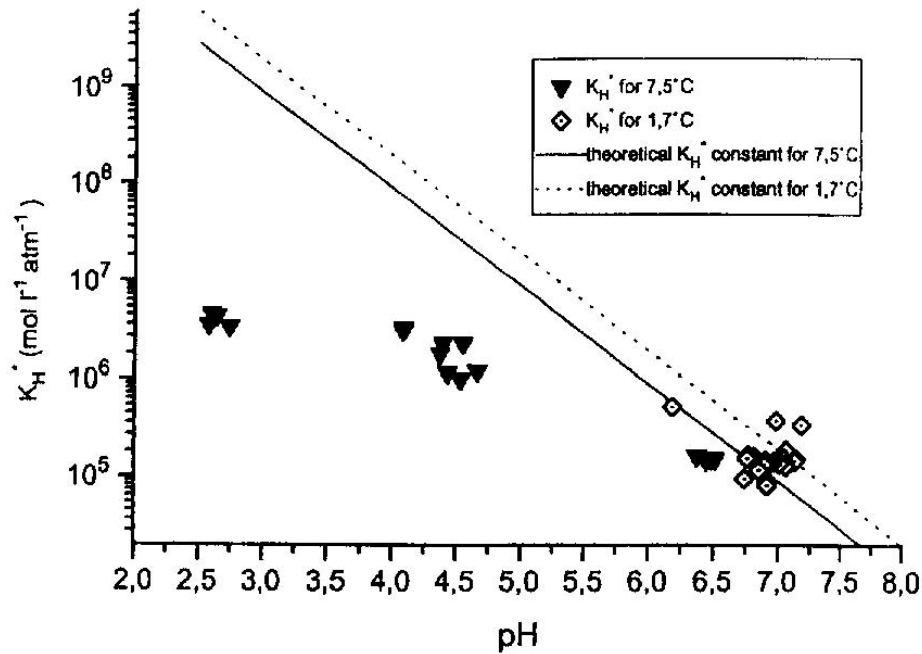


$$K_{\text{W}} = c_{\text{OH}^-} c_{\text{H}_3\text{O}^+} = 1.2 \times 10^{-14} \text{ M} \quad (298 \text{ K})$$

with: $K_{\text{A}} K_{\text{B}} = c_{\text{OH}^-} c_{\text{H}_3\text{O}^+} = K_{\text{W}}, (\equiv \text{p}K_{\text{S}} + \text{p}K_{\text{B}} = \text{p}K_{\text{W}})$

$$K_{\text{H NH}_3}^* = K_{\text{H NH}_3} (1 + c_{\text{H}_3\text{O}^+} / K_{\text{A}}) = K_{\text{H NH}_3} [1 + K_{\text{W}} / (c_{\text{OH}^-} K_{\text{A}})]$$

→ Verification of gas/aqueous partitioning and pH-dependency for fogwater
(Jaeschke et al., 1998)



Air and seawater $c_{N(-III)}$

Table 2. NH_3 Concentrations in Marine Areas^a

Location	NH_3 , nmol m ⁻³	Type	Reference
Central Atlantic Ocean, 15°N–5°S	3.7–18.4, (9.7)	Measurements	this study
	1–30	Measurements	<i>Zhuang and Huebert</i> [1996]
	20–35	Model	<i>Dentener and Crutzen</i> [1994]
	5–20	Model	<i>Quinn et al.</i> [1996]
Southern Atlantic Ocean, 5°S–35°S	0.1–7.7, (2.1)	Measurements	this study
	4–15	Model	<i>Dentener and Crutzen</i> [1994]
Southern Indian Ocean, 35°S–26°S	0.3–2.1, (1.1)	Measurements	this study
	2.2–4.4	Measurements	<i>Ayers and Gras</i> [1983]
	4–15	Model	<i>Dentener and Crutzen</i> [1994]
Central Indian Ocean, 26°S–15°S	0.05–0.2, (0.1)	Measurements	this study

Table 3. Summary of Data From the Four High-Latitude Cruises Presented Here, Along With Previous Studies in Similar Regions for Comparison^a

Cruise	Region	Season	($NH_{3(g)}$) nmol m ⁻³	Surface [$NH_{x(sw)}$] nM
PS211	NE Atlantic	autumn	1.4–8.0 (4.5)	90–450 (286) stdev = 87
S18/01	northern North Sea	winter	1.4–5.5 (2.9)	30–218 (72) stdev = 51
JR75	Norwegian Sea/Arctic Ocean	spring–summer	1.4–15.9 (7.5)	29–616 (146) stdev = 142
D267	Irminger Basin	winter	5.5–25.8 (n = 2)	17–217 (101) stdev = 95.7
Other studies	region	season	($NH_{3(g)}$) nmol m ⁻³	[$NH_{x(sw)}$] nM
<i>Johnson et al.</i> [2007]	NE Atlantic	spring	-	47–742 (266) stdev = 203
<i>Rees et al.</i> [2002]	northern North Sea	spring	-	30–70 (50)
<i>Rees et al.</i> [2001]	oligotrophic NE Atlantic (<50°N)	summer	-	55–110 (80)
<i>Asman et al.</i> [1994]	southern North Sea	Feb–Oct	2–88	300–4300 (~1000)
<i>Harrison et al.</i> [1993]	NW Atlantic	spring	-	80–300
<i>Ottley and Harrison</i> [1992]	southern North Sea	all seasons	6–35	-
<i>Edmunds</i> [1991]	southern North Sea	annual coverage	-	<500–32000 (1500)

^aData in parentheses are mean measured concentrations during each cruise/previous study.

(*Johnson et al., 2008*)

$c_{NH_3 \text{ gas}} > 1 \text{ nmol/m}^3$

$c_{N(-III) \text{ aqu}} < 100 \text{ nM}$ during periods of N limitation, lower levels in tropical seas

Seawater $c_{N(-III) \text{ aqu}} = f(T, \text{pH, ion strength})$:

T increases, pH decreases $c_{N(-III) \text{ aqu}}$

$$c_{\text{NH}_3 \text{ aqu}} = c_{\text{N(-III) aqu}} \frac{K_s}{(K_s + c_{\text{H}_3\text{O}^+})}$$

$$\text{p}K_s = -0.467 + (0.00113 S) + 2887.9/T$$

salinity S, temperature T

$$K_s/(K_s + c_{\text{H}_3\text{O}^+}) = 0.007 \text{ (273 K) and } 0.102 \text{ (303 K)}$$

$$K_{\text{aw}} = c_{\text{NH}_3 \text{ aqu}} / c_{\text{N(-III) aqu}} =$$

$$= [17.93 (T/273.15) e^{(4092/T - 9.70)}]^{-1}$$

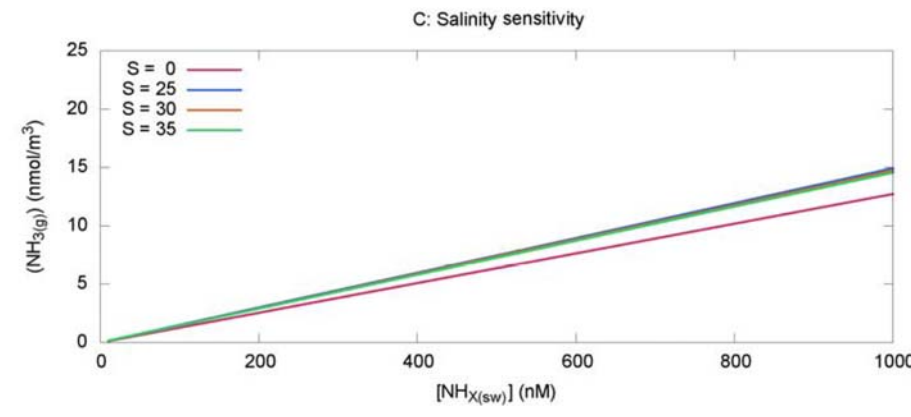
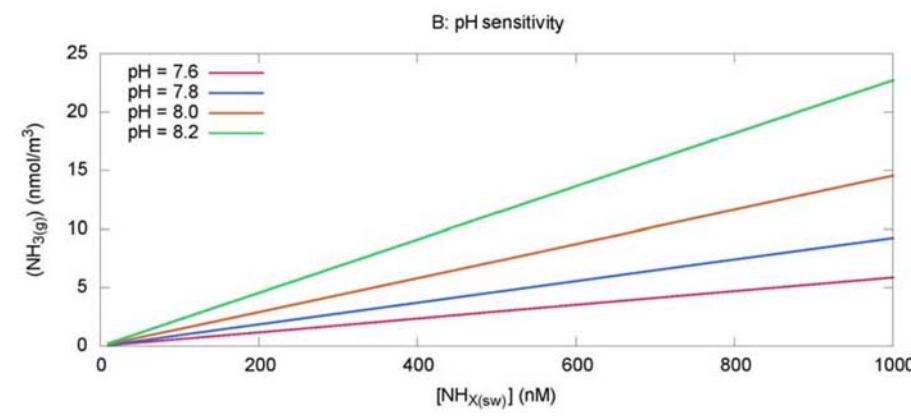
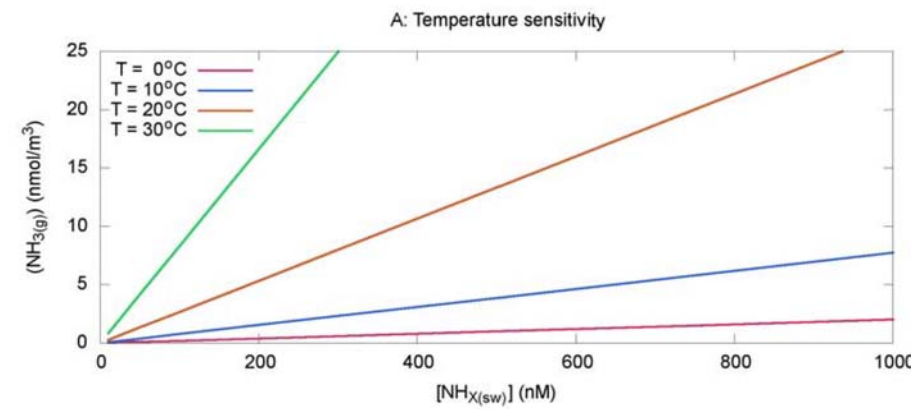
$$= 0.00028 \text{ (273 K) and } 0.0014 \text{ (303 K)}$$

air-water partitioning coefficient K_{aw}

These T-dependencies multiply!

A relatively small gas-phase concentration, $c_{\text{NH}_3 \text{ gas}} \approx 1 \text{ nmol/m}^3$, balances $c_{\text{N(-III) aqu}} \approx 100 \text{ nM}$ at $T \approx 283 \text{ K}$.

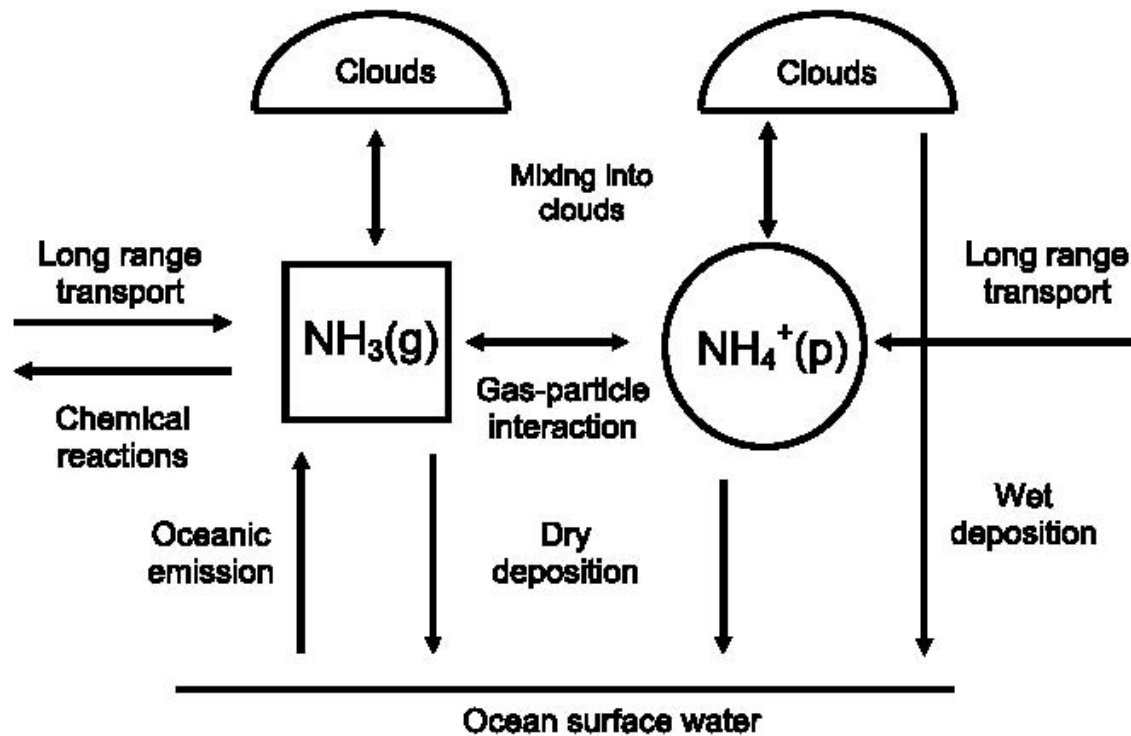
→ $c_{\text{NH}_3 \text{ gas}} = 1 \text{ nmol/m}^3 = 0.017 \text{ } \mu\text{g/m}^3 \approx \text{pptv}$ is difficult to measure.



(Johnson et al., 2008)

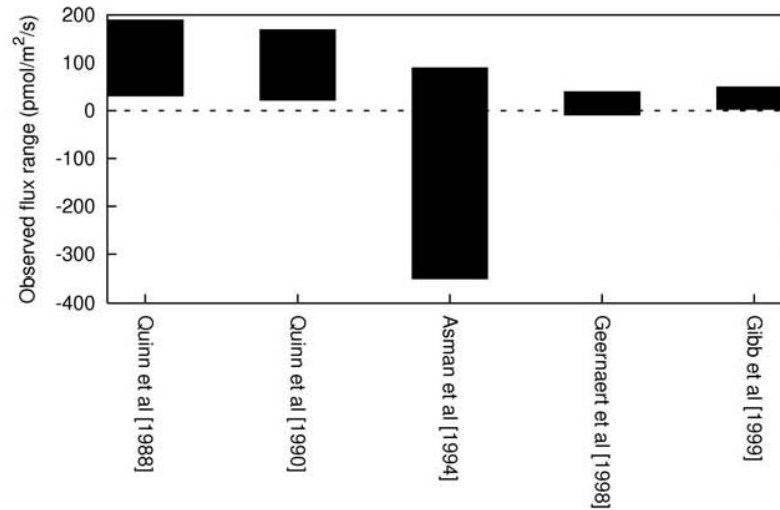
5.1.4.2 Fluxes

N(-III) cycling in the marine boundary layer (*Norman & Leck, 2005*)



+ is defined from sea to air
- from air to sea

Marine NH₃ sources



+ is defined from sea to air
- is defined from air to sea

(Johnson et al., 2008)

- Oceans are **NH₃ sources** (+ (5-8) Tg/a globally; continents ≈ 38) as biogenic NO₃⁻ is reduced. NH₃ is a volatile degradation product of organic N; *Quinn et al., 1996; Gibb et al., 1999*)
- c_{NH₄⁺} is high where NPP is high, low where NPP is low and nutrient-limited (efficient utilisation).
- Marine sources used in global modelling (e.g. *Dentener et al., 2006*) are based on a simplifying biogeochemical model. They are not corrected for non-zero c_{NH₃}.

Emission if:

$$c_{\text{NH}_3 \text{ aqu}} > c_{\text{NH}_3 \text{ (g)}} K_{\text{H NH}_3}^* = c_{\text{NH}_3} K_{\text{H NH}_3} (1 + K_{\text{B}} / c_{\text{OH}^-})$$

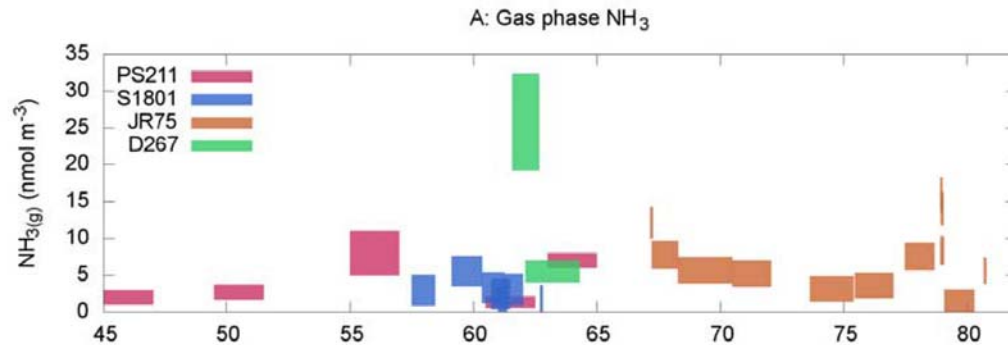
Oceans are **NH₃ sources** (+ (5-8) Tg/a globally; continents \approx 38) **but:**

In **air/sea exchange**, i.e. the net flux of dry deposition and volatilisation they are **net-receptors**:

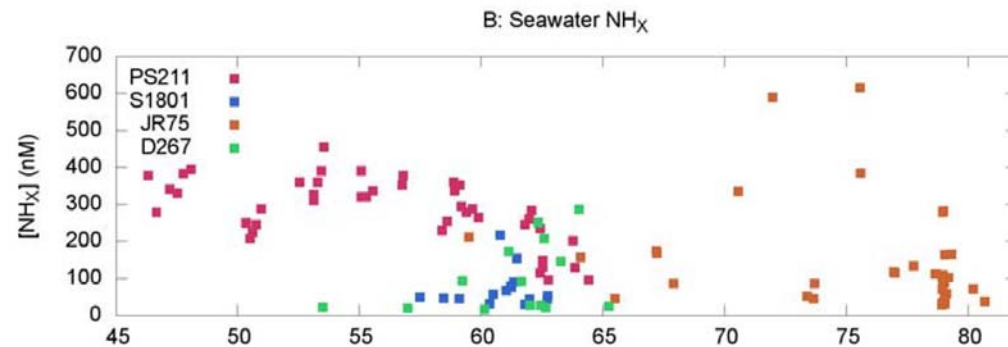
- because of T-dependency high-latitude seas are likely a net sink (despite high $c_{\text{N(-III) aqu}}$)
- historically since \approx 1860: Oceans were net emitters of NH₃ in the anthropogenically undisturbed past: source of 1-4 Tg/a in 1860 (pH was higher than today's), then turned into net-receptors by 1860 (continental sources were at \approx 9 Tg/a) and even more so since then (*Galloway et al., 1995*)
- supported by isotopic signature of NH₃(g) (very low ¹⁵N content of marine biogenic N; *Jickells et al., 2003*)
- future trend: net depositional flux, -(5-1.5) Tg/a, is expected as the air/sea exchange $\text{N(-III)}_{\text{sea}}/\text{N(-III)}_{\text{air}}$ for $\Delta\text{pH} = -0.4$ and $\Delta T = 2.0$ K (*Johnson, 2004*)

Uncertainty of flux determination: measure NH_3 (g), NH_4^+ part. and $\text{N(-III)}_{\text{aqu}}$
However: long integration times of measurement (common) are inadequate as seawater ammonium concentrations are highly variable, especially in summer:

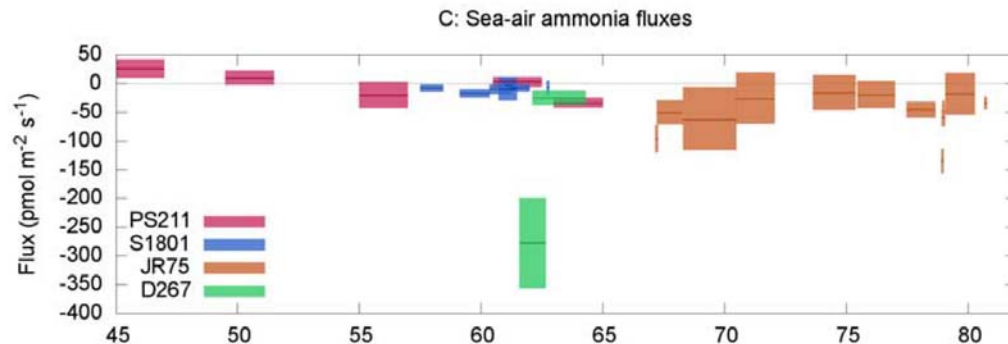
→ uncertainty associated with the integration of seawater measurements over the



long integration times translate into large spatial uncertainty



significant variability



(Johnson et al., 2008)

Revisited (→ 3.3.4.2):

Hypothetical neg. feedback mechanism in the marine boundary layer (so-called CLAW hypothesis):

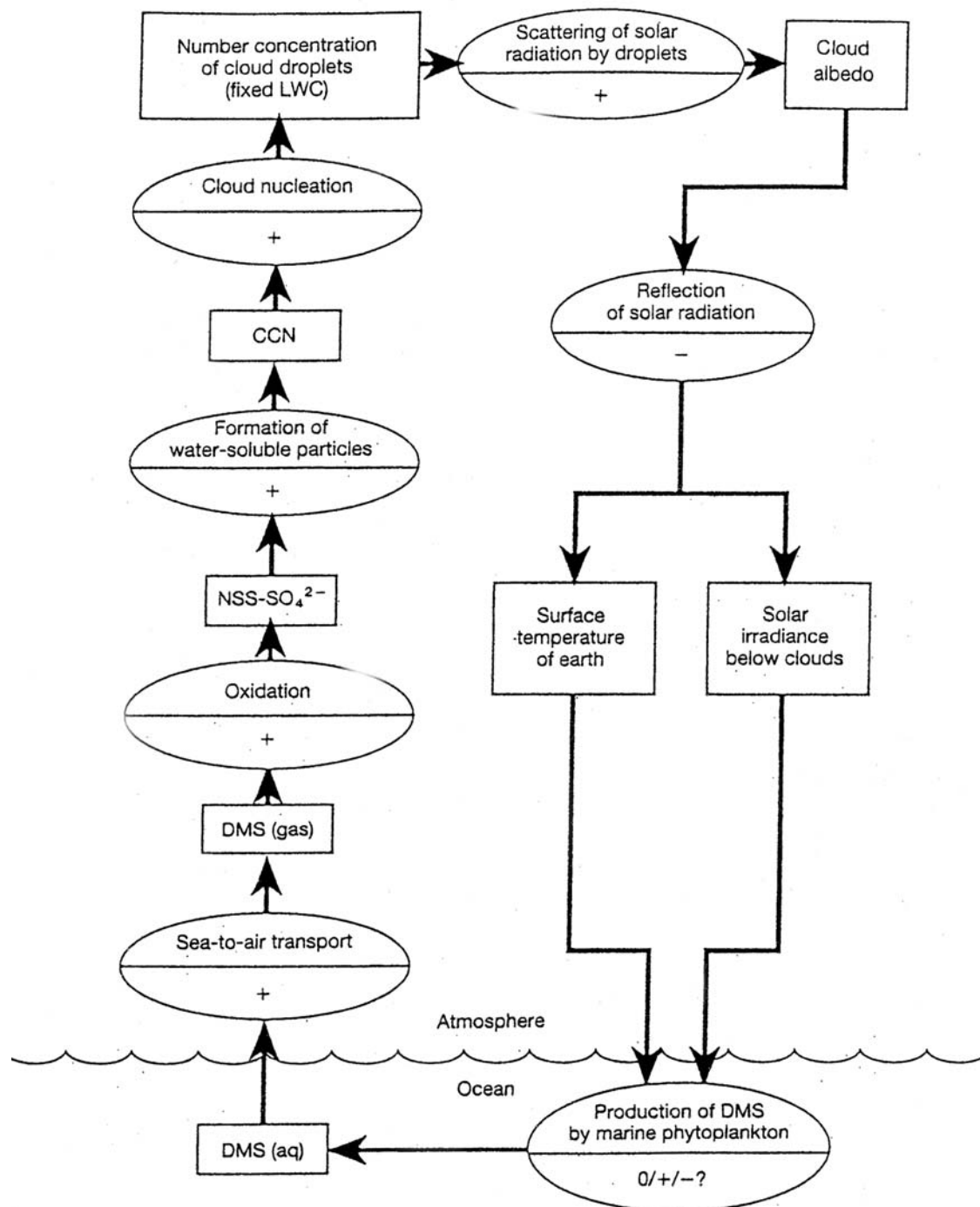
$\text{CH}_3\text{SCH}_3 \rightarrow \text{clouds} \rightarrow$
 $\text{radiation} \rightarrow \text{phytoplankton}$

→

(Charlson et al., 1987)

CH_3SCH_3 production
coupled with NH_3 ?

(Quinn et al., 1988, besides others)

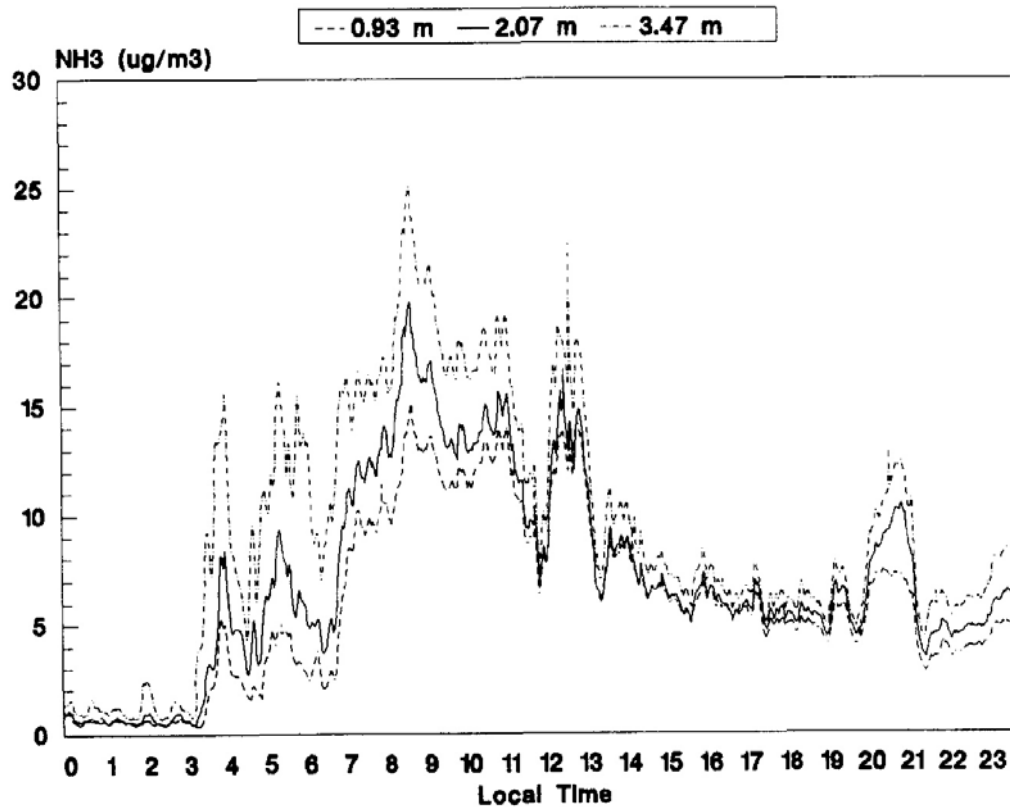


Ammonia trends and questions

- Due to air pollution policies $\text{NH}_4^+ / (\text{SO}_4^{2-} + \text{NO}_3^-)$ ratio is increasing in depositions, which will add to nutrient surplus and will not change acidification trends in soils.
- NH_3 global emissions are expected to increase (agriculture) - despite the fact that air/sea exchange, $\approx 5-8 \text{ Tg/a}$, is expected to be turned into $(-1.5-5) \text{ Tg/a}$.
- Consistent chemistry-climate model studies not available. Whether gas/particle partitioning and, hence, atmospheric residence time will change is unclear. How good do we know Δrh ?

5.1.5 Ammonia surface fluxes

Vegetation canopies

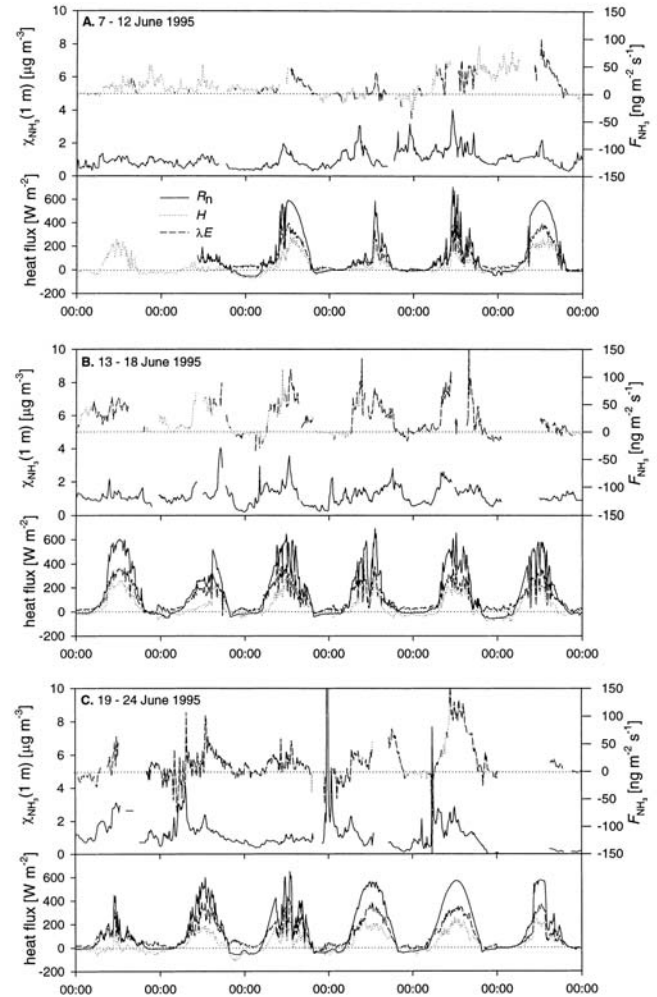
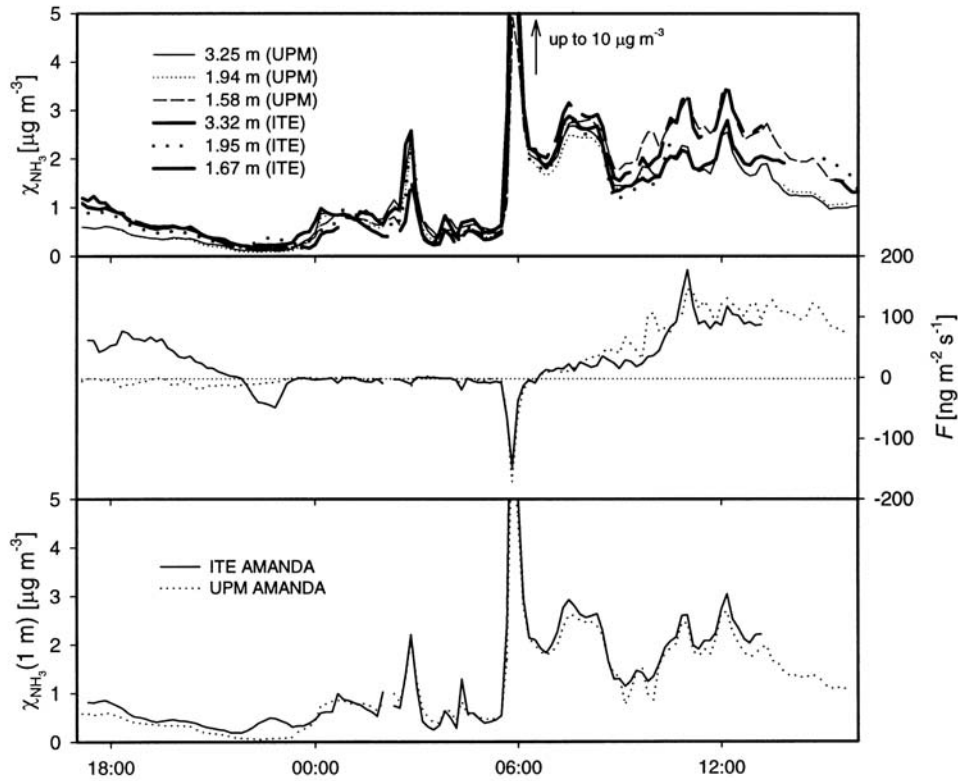


(Wyers et al., 1993)

NH₃ gradient over a heather canopy, Leende/NL, 1991

Data interpretation: via flux-profile relationships

- Sampling proportional to wind velocity passive, i.e. wind driven
- Denuder active sampling:



(Sutton et al., 2000)

9.3.2 Flux measurement

In the lowermost tens of meters of air (constant-flux layer, CFL) fluxes are in steady state as the concentration of a conservative (inert) tracer is determined by vertical exchange only which, in turn, is the combination of turbulent mixing, convection and molecular diffusion.

9.3.2.1 Gradient method

The vertical concentration gradient of the gas under study is measured over the surface where exchange is occurring and effectively integrates over an area or 'fetch' extending upwind of the measurement site. The flux F is related to the gradient via the diffusion constant k in analogy to molecular diffusion

$$F_i = -K_z \Delta c_i / \Delta z \text{ (Fick's 1st law)}$$

with: Vertical turbulent diffusion coefficient (or Eddy diffusivity) K_z ,
Height above surface z ,
Gradient $\Delta c / \Delta z$ (> 0 for emission, < 0 for deposition)

K_z needs to be determined by

- micrometeorological measurements (directly) or by
- the flux and gradient of a reference quantity, e.g. heat, CO_2 :

$$F_j = -K_z \Delta c_j / \Delta z$$

$$F_i = F_j \Delta c_i / \Delta c_j$$

Reference quantity heat:

$$F_i = K_i \partial c / \partial z \approx F_i = K_h \partial T / \partial z$$

- for large surface sources
- applicable in the absence of fast sensors (measure Δc , Δu)

$$\rightarrow \rightarrow F_i = -kz u_* / \varnothing_h \partial c / \partial z \approx k / \varnothing_h u_* \Delta c / \ln(z_2 / z_1)$$

with: *von Karman* constant $k \approx 0.4$,

reference height z

$$\text{friction velocity } u_* = -kz / \varnothing_m \partial u / \partial z \approx k / \varnothing_m \Delta u / \ln(z_2 / z_1)$$

empirical functions of the *Monin-Obukhov* similarity parameter, $\xi = z/L$ (*Monin-Obukhov* length L), for the heat and momentum fluxes \varnothing_h and \varnothing_m

heights above surface z_i

vertical gradient Δc

Monin-Obukhov theory predicts the well-known log-linear form of the vertical wind speed profile.

$$\varnothing_h = \varnothing_m^2 = (1 - 15\xi)^{-1/2},$$

for $-5 < \xi < 0$ (unstable)

$$\varnothing_h = \varnothing_m = (1 + 5\xi),$$

for $0 \leq \xi < 1$ (stable)

$$\varnothing_h = 1 + [(1 + 0.667\xi)^{1/2} + 0.667 (6 - 0.35 \xi) e^{-0.35 \xi}] \xi$$

$$\varnothing_m = 1 + [1 + 0.667 (6 - 0.35 \xi) e^{-0.35 \xi}] \xi,$$

for $\xi \geq 1$ (very stable)

(*Arya, 1995, 2001; Beljaars & Holtslag, 1991*)

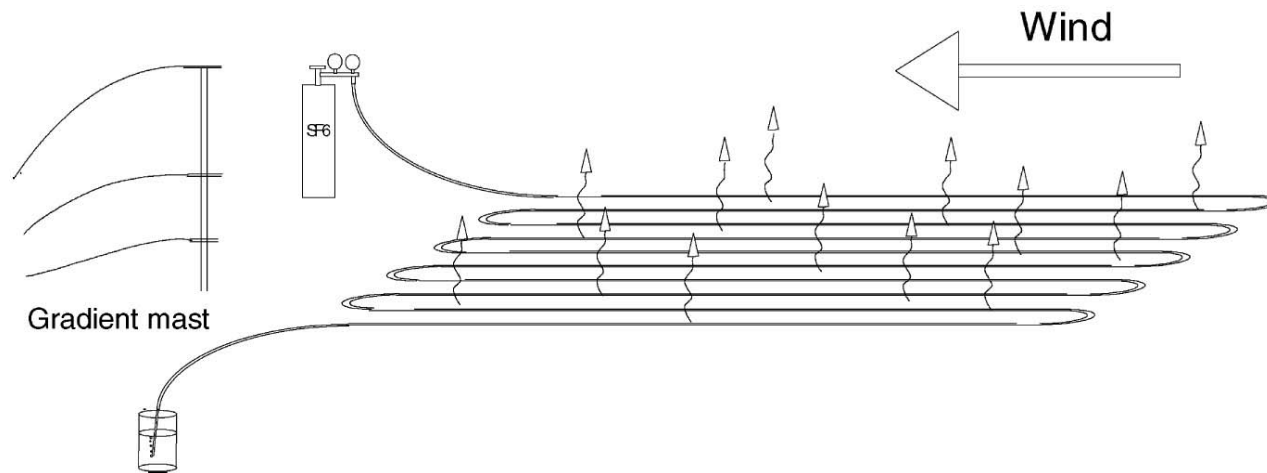
Further flux measurement methods for ammonia: FTIR

Gradient measurement using an area-averaging technique, FTIR

High sensitivity using a long optical path by means of multiple reflection optics (e.g. White cell)

$$F_{\text{NH}_3} = -K_z \Delta c_{\text{NH}_3} / \Delta z$$

$$F_{\text{NH}_3} = F_{\text{SF}_6} \Delta c_{\text{NH}_3} / \Delta c_{\text{SF}_6}$$



(Galle et al., 2000)

Other micrometeorological measurements: Single height

9.3.2.2 Eddy accumulation

Single height, no fast response necessary (usually not feasible with chemical sensors):

Eddy accumulation (EA, or: conditional sampling): not simultaneous but separated sampling in two reservoirs according to sign of w .

However: sampling proportional to wind velocity

which requires fast-response proportional sampling valves (or passive, i.e. wind driven)

9.3.2.3 Relaxed Eddy Accumulation (REA)

Businger & Oncley, 1990

EA but collecting at constant rate. If $w \approx 0$ (*Hicks & MacMillen, 1984*):

$$\begin{aligned}\overline{w^+ c} + \overline{w^- c} &= \overline{w^+ (\bar{c} + c')} + \overline{w^- (\bar{c} + c')} \\ &= (\overline{w^+} + \overline{w^-}) \bar{c} + \overline{w^+ c'} + \overline{w^- c'} \\ &= \overline{w^+ c'} + \overline{w^- c'} \\ &= \overline{w' c'}.\end{aligned}$$

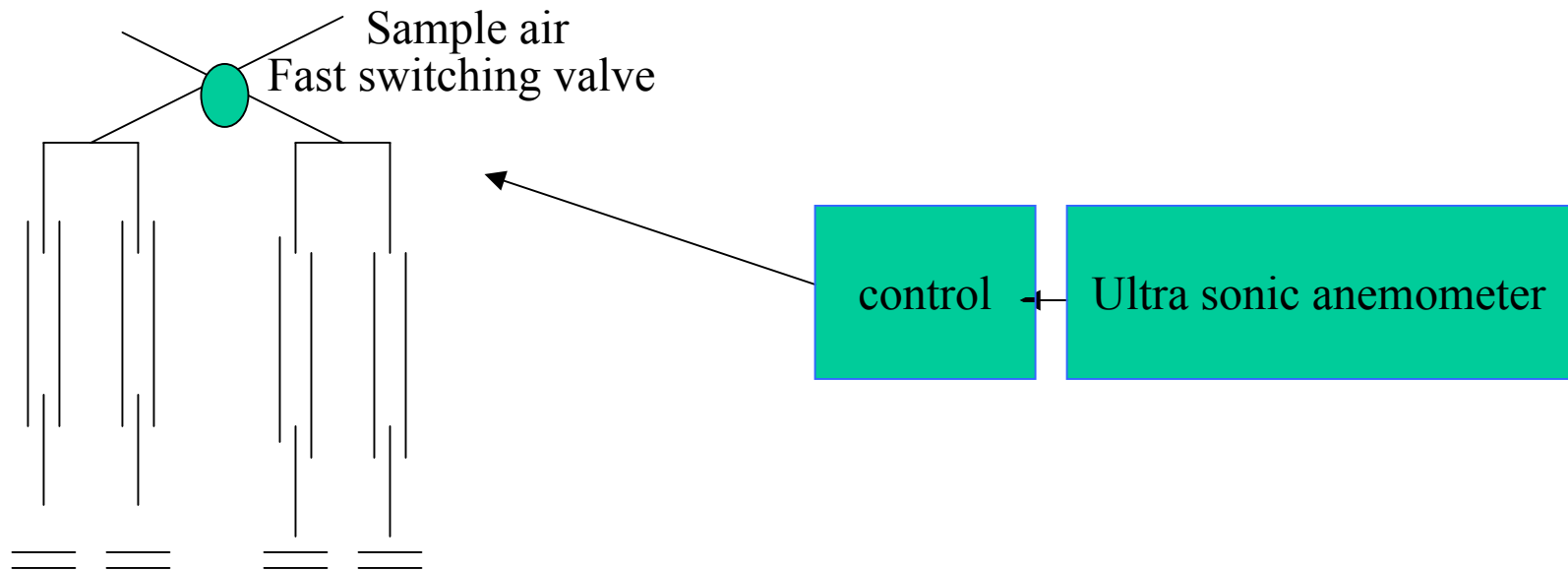
One integrating sampler measures during updrafts ($\rightarrow c^+$), another during downdrafts ($\rightarrow c^-$) and the difference is used to estimate the net flux.

One integrating sampler measures during updrafts ($\rightarrow c^+$), another during downdrafts ($\rightarrow c^-$) and the difference is used to estimate the net flux.

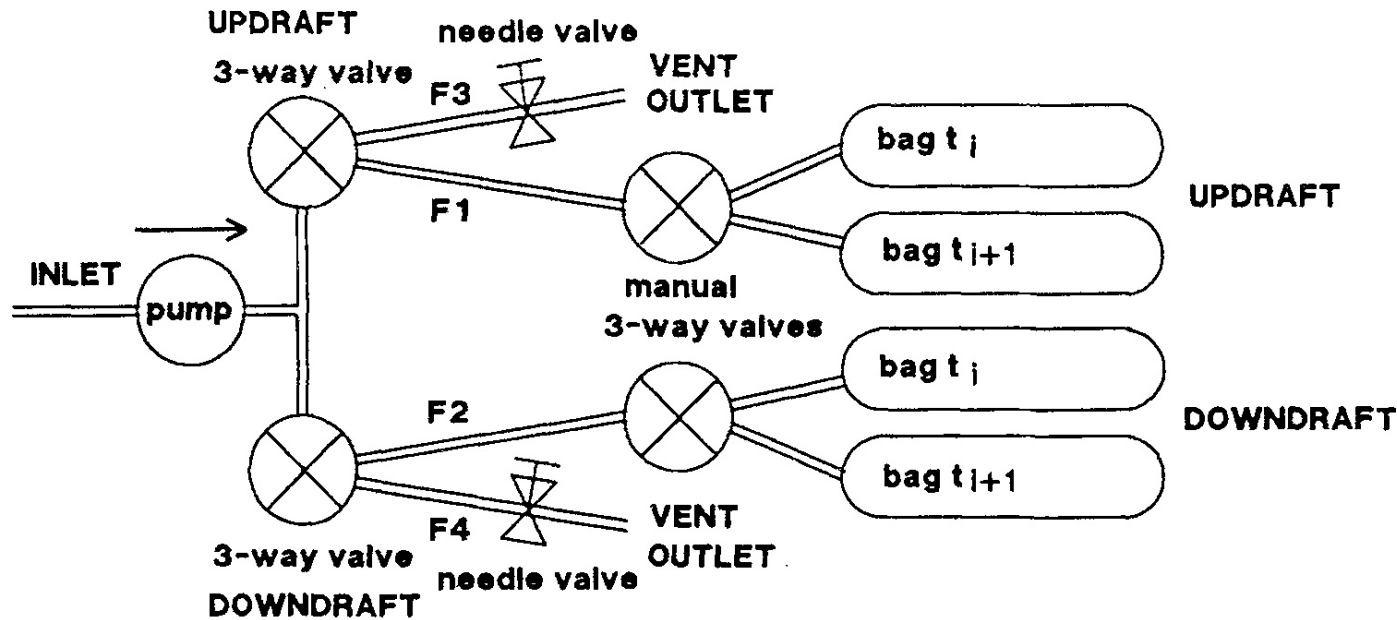
$$F = \beta \sigma_w (c^+ - c^-), c^+ \approx c^-$$

with: standard deviation of vertical wind component σ_w ,

empirical factor $\beta = 0.58 \pm 0.02$ over smooth surfaces, ≈ 0.5 close to canopy top
(e.g. *Gao, 1995*)



2 pairs of denuders and filter packs (e.g. T, N + W for N(V) / N(-III) measurements)



FLOW	F1	F2	F3	F4
$+D < W$	1	0	0	1
$-D \leq W \leq +D$	0	0	1	1
$W < -D$	0	1	1	0

The status of flows F1 to F4 indicates if there is a flow (1: yes, 0: no) through the tubing depending on the vertical wind velocity (W) compared to the negative and positive value of the deadband ($\pm D$). Air is collected in bags that are changed from one period (t_i) to another (t_{i+1}). (Pattey et al., 1993)

9.3.2.4 Eddy covariance

$$F = \overline{wc} = \overline{w'c'}.$$

Measuring the covariance

as $\bar{w} \approx 0$

Mean product of the fluctuations of vertical wind velocity and trace substance concentration

Single height only but fast:

temporally high-resolved (≥ 10 Hz) measurement of concentration and vertical wind component.